FEASIBILITY OF ELECTRIC FIELD SENSOR FOR EXTERNAL BALLISTICS ANALYSIS

by

Christopher John Benfield

A thesis submitted to the faculty of
The University of North Carolina at Charlotte
in partial fulfillment of the requirements
for the degree of Masters of Science in
Applied Energy and Electromechanical Systems

Charlotte

2014

Approved by:

_____
Dr. Wesley Williams

_____
Dr. Maciej A. Noras

_____
Dr. Peter Schmidt

ABSTRACT

CHRISTOPHER JOHN BENFIELD. Feasibility of electric field sensor for external ballistics analysis. (Under the direction of DR. WESLEY WILLIAMS)

Accurately modeling the flight path to resemble the actual flight dynamics of a given projectile enables a shooter to engage targets at distances that extend into the transonic and subsonic flight regions. This requires the collection of velocity measurements of the actual projectile at several points along the flight path. Current methods for collecting velocity measurements have accuracy and consistency limitations or become cost prohibitive.

The electric field sensors evaluated in this thesis seek to provide a highly accurate cost effective means of collecting velocity readings at all ranges and flight regions. The electric field sensors detect the static charge of the projectile as it passes the sensor location. To gather velocity measurements two sensors are placed in a linear array with a measured distance between them and projectile are fired over the sensor detection plates. The detections appear as voltage spikes that are captured using a trigger on the data acquisition device. The time difference between the peaks of detection provide an accurate velocity measurement that is within 2% of optical chronograph referenced values for the same projectile firing event.

The sensors used for testing started to develop issues in consistently detecting and producing voltage peaks that could be used for velocity measurements. The conclusion was reached that a portion of the internal circuitry was gathering and holding a charge, reducing the sensors ability to detect passing projectiles. To continue testing, a reconfiguring of the sensors toward a prior embodiment is recommended.

ACKNOWLEDGMENTS

I would like to thank my adviser, Dr. Wesley Williams, for his patience, his guidance, his ideas, and his faith in my abilities. I have grown both professionally and personally under his guidance. I would also like to thank the other members of the supervisory committee; Dr. Maciej A. Noras for enabling this research by making the sensors and his expertise available. I hope that this research serves to advance what is already a worthy and useful tool. Dr. Peter Schmidt for asking the challenging questions and ensuring the integrity of the work.

Sincere thanks is due to my Aunt, Margaret Vernum for facilitating a suitable location for high velocity testing.

Special thanks to my family for supporting me through all the frustrations and late, late nights involved in completing this endeavor. I could not have done it without you.

TABLE OF CONTENTS

CHAPTER 1: INTRODUCTION

The purpose of this research was evaluating the suitability of electric field sensors as a means of investigating the uncertainties in exterior ballistics inherent in all revolving, gyroscopically stabilized projectiles. These uncertainties include: the drag coefficients of projectiles in various stages of the transonic flight region and the need for increased accuracy in determining the velocity of the projectile at the muzzle. Each of the above uncertainties increases the difficulty in striking a distant target with a high hit percentage. Mitigation of these uncertainties allows for accurate prediction of the actual flight path and an increase in hit percentage at extended ranges.

Through adherence to tolerances in the manufacturing processes and consistency in the powder loading process of ammunition, key variables that negatively affect the accuracy potential of a rife – ammunition combination (weapon system) are mitigated. The difficulty in collecting velocity measurements with minimal error, specific to the weapon being employed, can hinder its effective employment at increased ranges.

Ballistic algorithms used in the formulation of projectile flight solutions are only capable of producing accurate results when supplied with accurate input data. Figure 1 shows how the likelihood of striking a distant target is reduced, given varying levels of uncertainty in muzzle velocity. At 800 yards a difference of 10 feet per second (fps) standard deviation in muzzle velocity can reduce the probability of striking a target from

80% to roughly 55%. The decreased hit percentage from 700 – 1300 yards coincides with the projectile entering and exiting the transonic flight region.

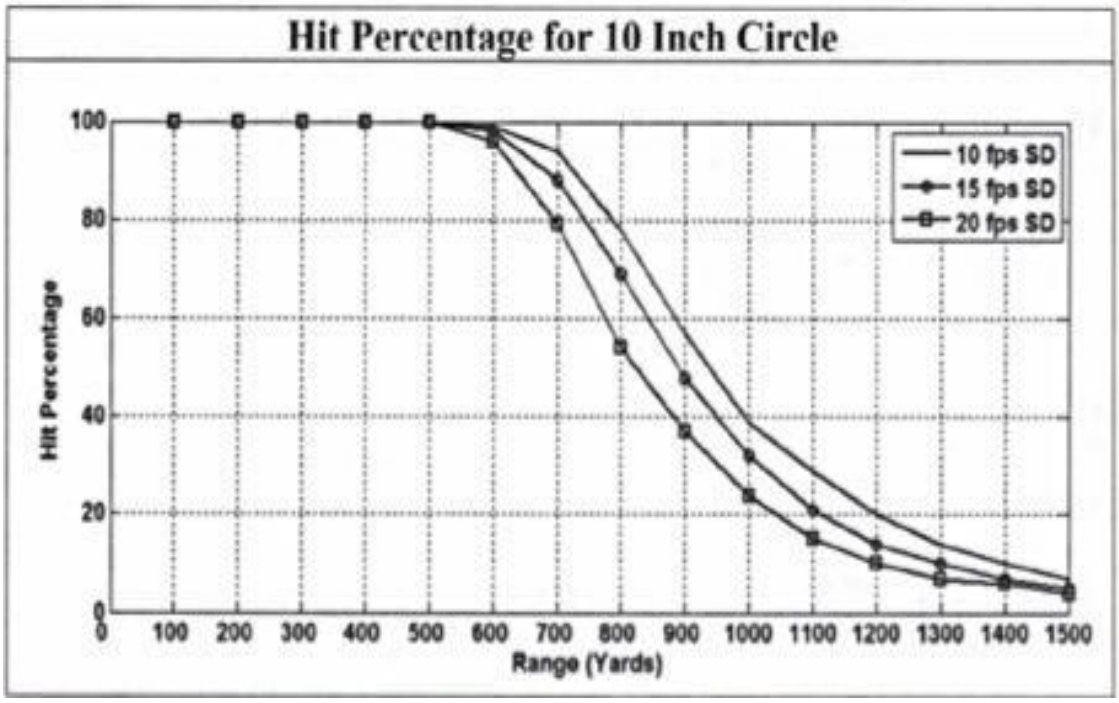

Figure 1: Hit percent by standard deviation in muzzle velocity [4]

Current methods for velocity detection suffer from inconsistencies in velocity measurements, inabilities to capture velocity readings in the transonic and subsonic region, and cost restrictions. By gathering more accurate data on muzzle velocity and downrange velocity readings, the hit percentage, especially when the projectile is transonic, can increase significantly.

Research focused on testing, evaluating, and refining sensors developed by Dr. Maciej A. Noras [9] at the University of North Carolina Charlotte with development and testing help from the Army Research Laboratories in Aberdeen, Maryland. The sensors detect electric field perturbance created by the passing of charged projectiles.

The sensor's detection was employed to record time of flight differences between detection by the lead and second sensor. This time difference was used to calculate the velocity of the projectile at any given point along the flight path. With the ability to accurately determine velocity established, the research shifted to increasing the consistency and dependability of detections.

CHAPTER 2: THEORY AND LITERATURE REVIEW

2.1 External Ballistics

2.1.1 History

The development of ballistics as a true science began shortly after firearms were introduced into warfare in Western Europe, around the 15th century. Some of the greatest scientist and mathematicians in history are associated with the development of ballistics, including Leonardo da Vinci, Galileo, and Isaac Newton. Through their work, and that of others, the conclusion was reached that a bullet traveling through the air is acted on by two distinct forces: The force of gravity being constant and the force of air flowing around the body causing drag and deflection when perpendicular to the flight path. After a projectile leaves the barrel, the trajectory is determined completely by these factors. [2]

2.1.2 Variables

Several variables affect the flight characteristics of revolving projectiles and have a profound effect on accuracy and precision. These variables are described as deterministic and non-deterministic. [4]

Deterministic variables are those that can be readily measured and controlled. Most variables involved in the study of revolving projectile flight fall into this category. The constant effects of gravity and drift associated with revolving projectiles are two examples of deterministic variables. [4]

Non-deterministic variables are extremely hard to measure directly. These variables can have a dramatic effect on the accuracy and precision of the projectile's flight path. [4] Wind and variance in initial (muzzle) velocity are two of the biggest non-deterministic variables affecting trajectory of the projectile. The operator has no control over the natural effects of wind on projectile flight. The best approach is to generalize the effect and compensate accordingly. Variance in muzzle velocity can be reduced through the careful preparation of the components used to launch the projectile. In practice, when considering two weapons of identical make and model, the same type of projectiles often leave the barrel at different velocities, leading to a different amount of drop at extended range. [4] To account for these effects, the measurement of muzzle velocity for a particular rifle and ammunition type (weapon system) must be as accurate as possible.

2.1.3 Projectile Flight Regions

From the instant the projectile leaves the barrel it is decelerating. Depending upon the initial velocity, the projectile will experience either single or multiple flight regions. These flight regions exert different drag forces upon the projectile that in turn vary the amount of deceleration. Flight regions are classified by the characteristics of the air flowing around the projectile. True supersonic flight (> Mach 1.05) indicates that presence of pure supersonic flow over the projectile, transonic flow (approx. Mach 1.05 - Mach 0.85) indicates air flow around the projectile that changes from supersonic to subsonic depending on geometry changes and velocity decay, and subsonic (< Mach .85) indicates pure subsonic air flow around the projectile. [6] Figure 2 shows the drag coefficient (Cd) of a typical long rage projectile through various flight regions.

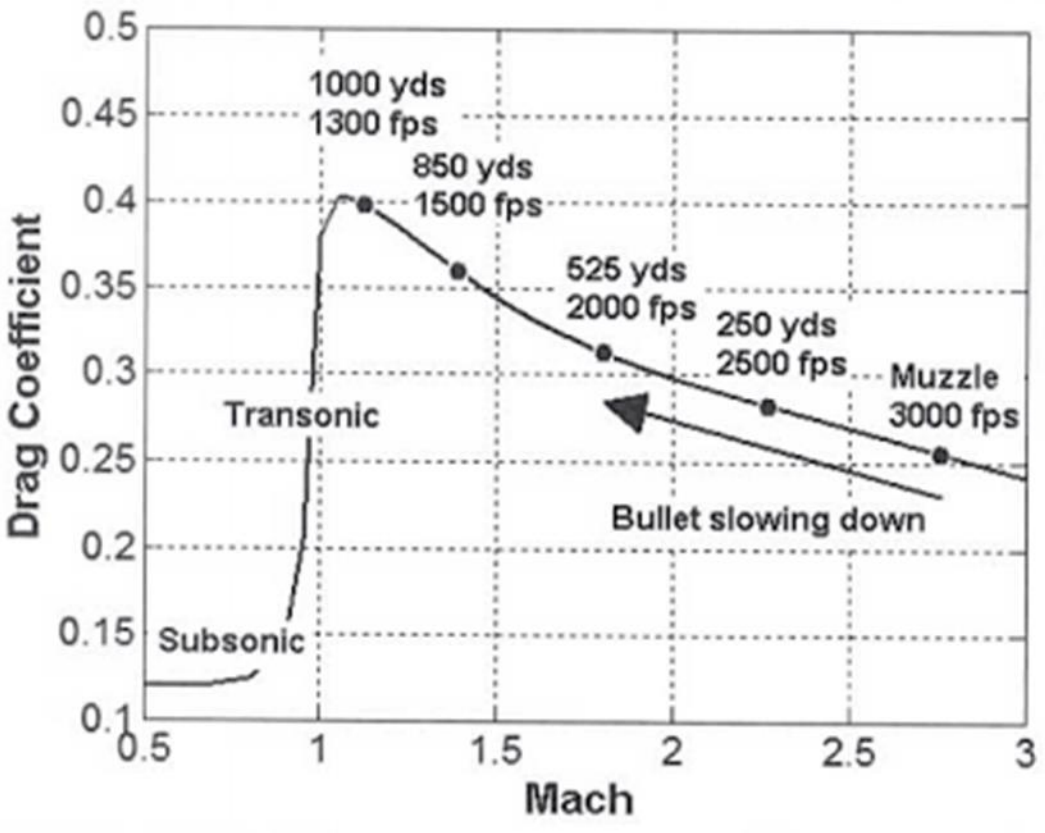

Figure 2: Drag curve for a typical long range bullet [4]

The following sections characterize the flight regions of revolving projectiles. The specific projectile used in the figures is a 0.510 inch diameter, 670 grain M33 ball projectile. The projectiles shape characteristics are describe in figure 3.

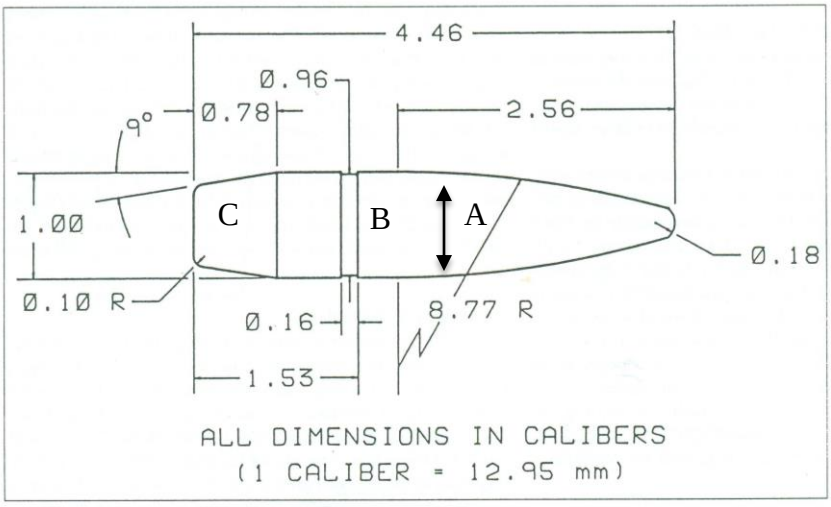

Figure 3: Caliber .50 ball M33 projectile [6]

Where: A is the ogive intersection, B is the full bore diameter section, and C is the boat tail area.

2.1.4 Supersonic Flight

This region of flight is characterized by the entire envelope of air surrounding the projectile being fully supersonic. Full supersonic flow indicates that the air passing over the projectile has been fully compressed and the projectile rides in the smooth wake of the bow shock wave as seen in figure 4. [6]

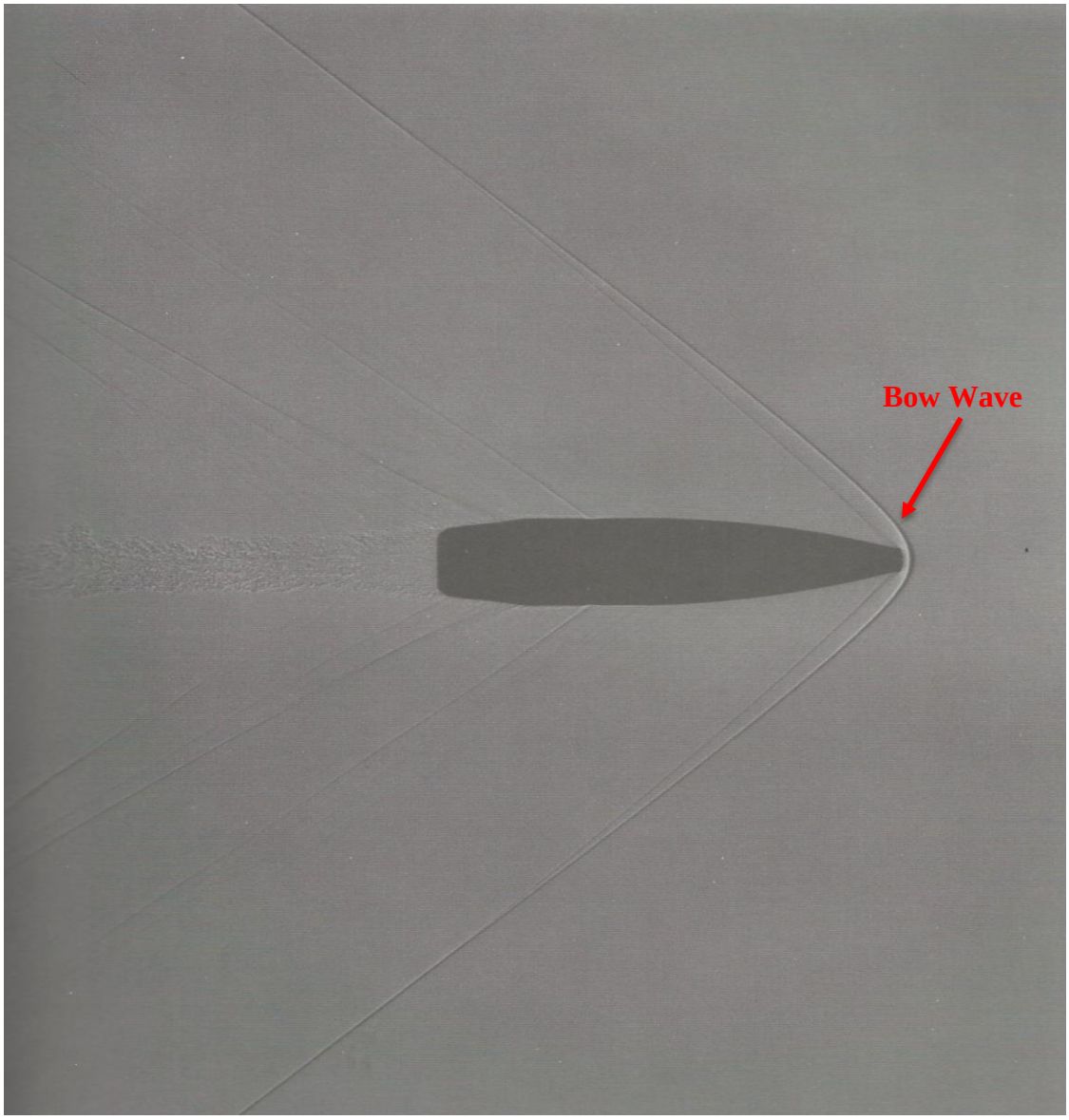

Figure 4: Field flow of caliber .50 ball M33 at Mach 1.53 [6]

As the projectile slows and approaches the transonic flight region (approx. Mach 1.5 – 1.05) the drag coefficient (Cd) begins to rise sharply. The sudden rise in Cd is caused by the formation of shock waves in the flowfield around the projectile. In the projectile shown in figure 5 the bow wave starts to move away from the projectile as the air in front of the nose begins to decelerate below supersonic. This occurs in part due to

the geometry of the nose and the compressibility of air. The Cd of 0.365 at this velocity is near maximum value. [6]

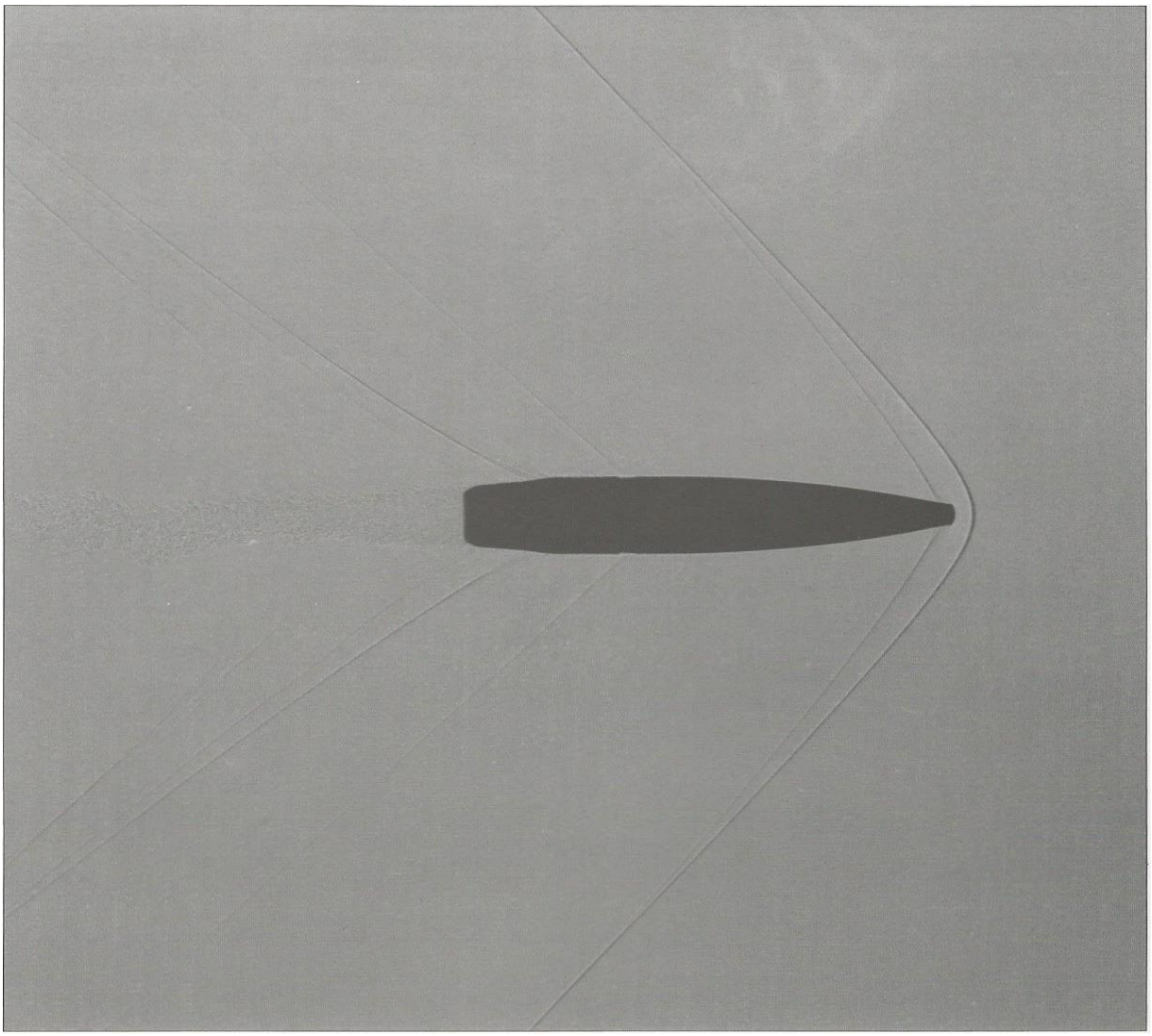

Figure 5: Field flow of caliber .50 ball M33 at Mach 1.24 [6]

2.1.5 Transonic Flight

A projectile launched at supersonic velocities (>1340 fps) and unassisted by internal propulsion will experience much the same effects of aircraft as they transition from supersonic to subsonic flight (< 890 fps). Since a bullet is shaped like a wedge, it creates local regions of supersonic air flow even when the projectile is actually flying at

near subsonic velocities. This effect occurs due to the compressibility of air. The range of flight speeds where the airflow around the bullet is transitioning from compressible (fast) to incompressible (slower) is known as the transonic flight regime [4] Figure 2 in the previous section displays the drastic changes in drag coefficient propagated by the deterioration of velocity from the supersonic through transonic and into the subsonic region.

This dramatic change in drag coefficient is not instantaneous, but comprises a significant portion of the projectiles total flight. Figure 6 was created by using an external ballistics solver from Berger Bullets to plot the velocity along the flight path of a .308 inch diameter 150 grain projectile.

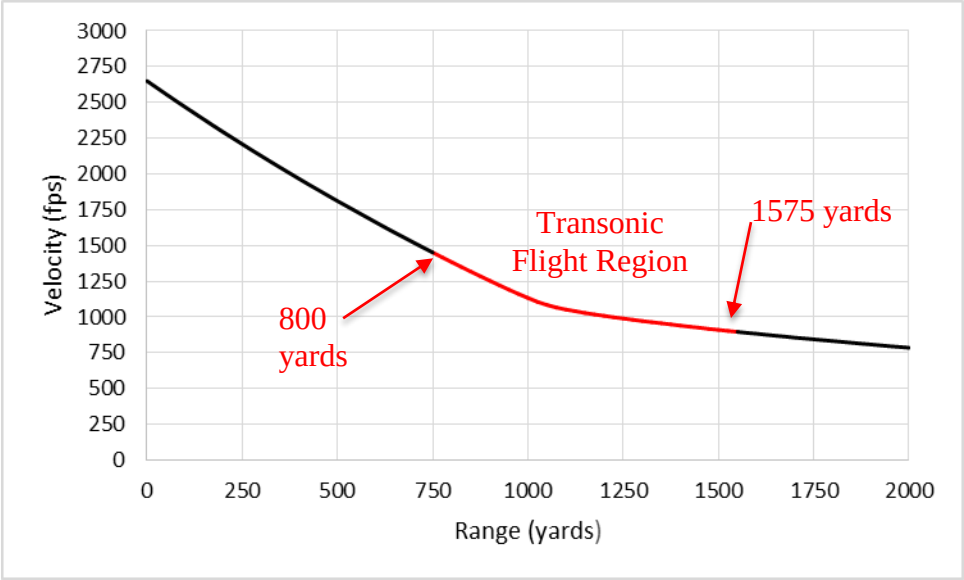

Figure 6: Velocity at range for .308" dia. 150 gr. projectile

Figure 7 shows the flow over a projectile at the start of transonic flight. The air passing over the front portion of the projectile is in subsonic flight as the rear portion is maintaining supersonic flow as indicated by the trailing shock wave.

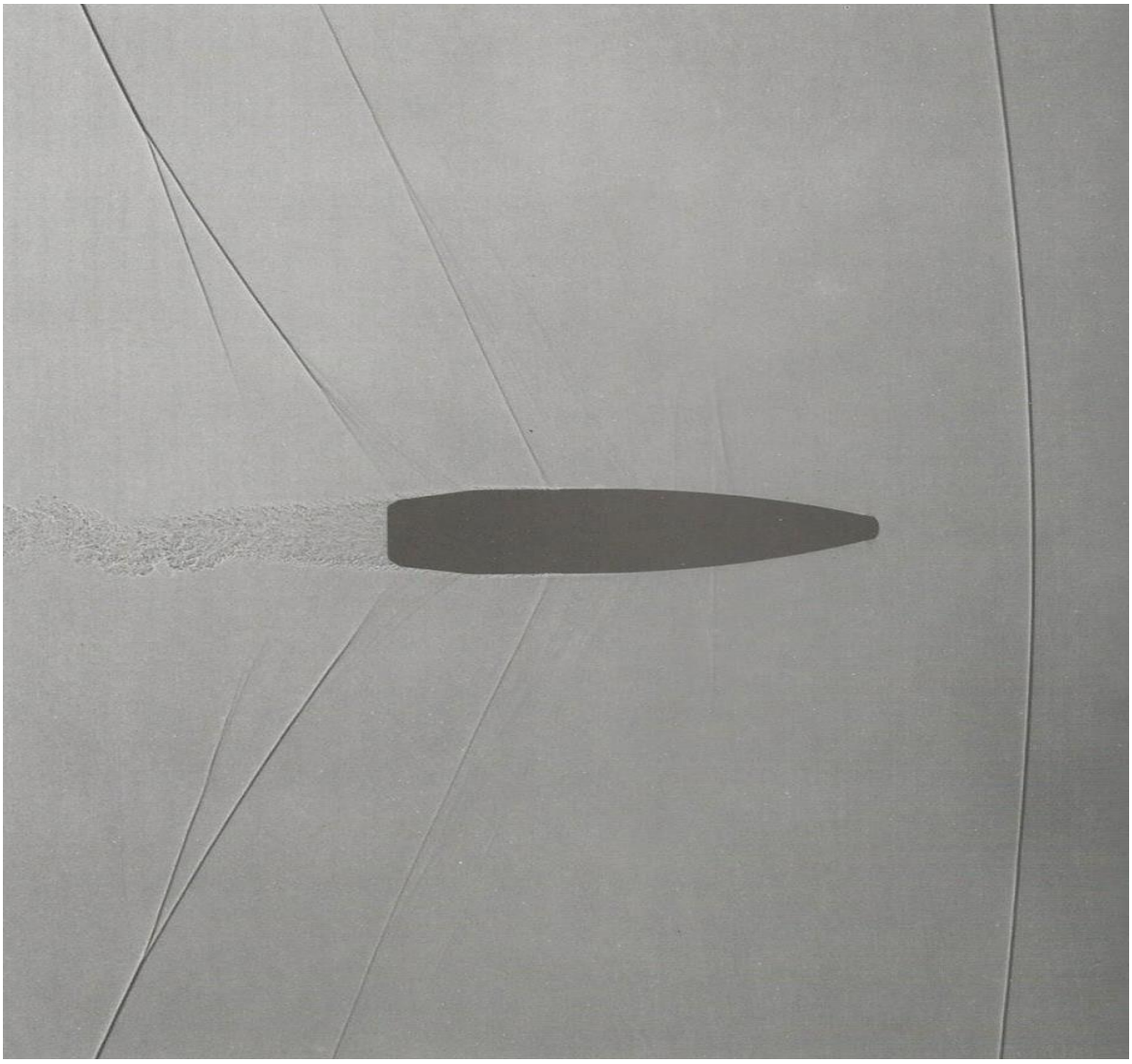

Figure 7: Field flow of caliber .50 ball M33 at Mach 1.02 [6]

Figure 8 shows the projectile at the mid stages of deceleration through the transonic region. The flow over the front portion of the projectile is subsonic. When the ogive of the projectile ends it creates a localized area of supersonic airflow. Changes in the profile continue to change the flow regime from supersonic to subsonic for the length of the projectile. [6]

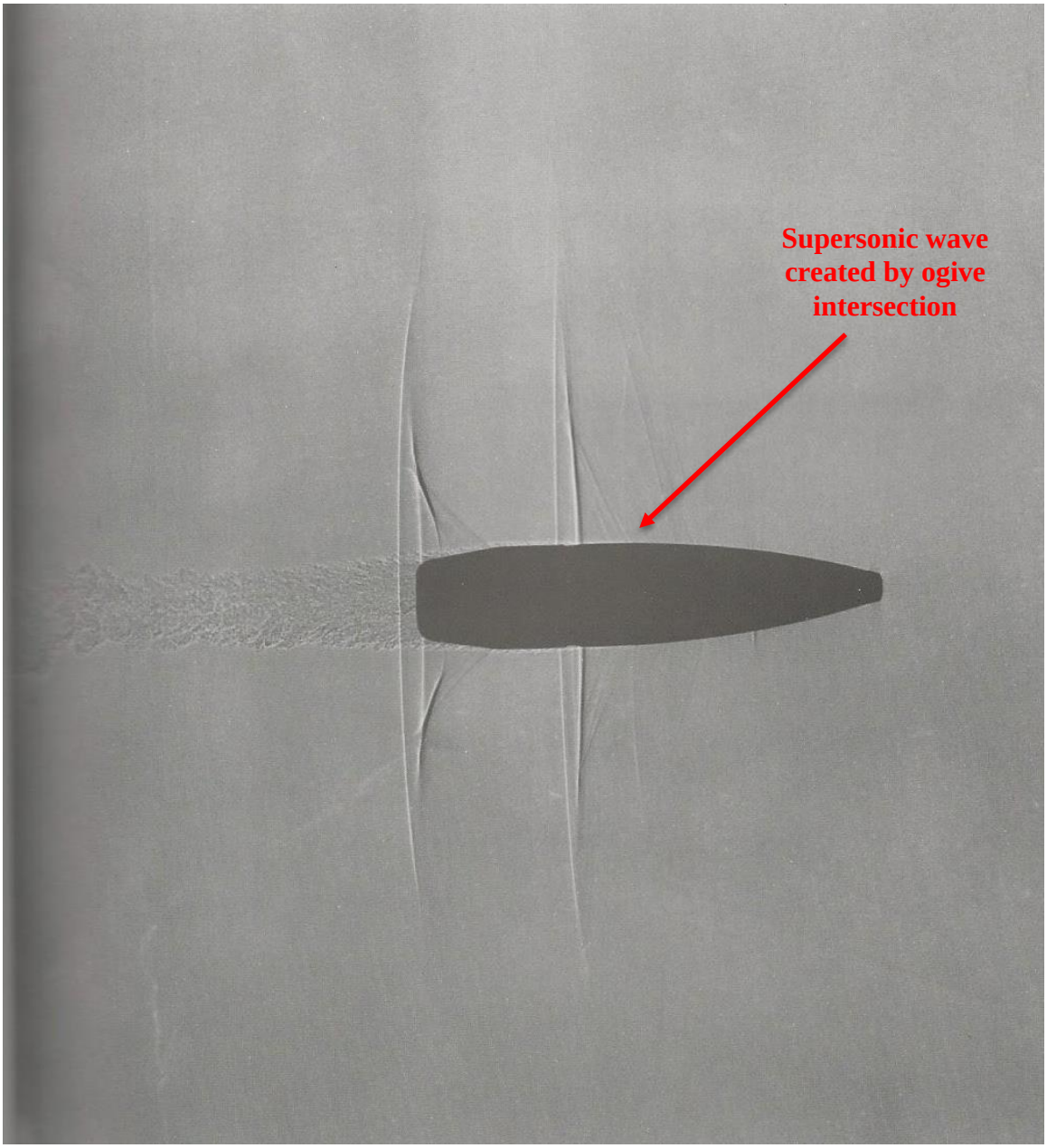

Figure 8: Field flow of caliber .50 ball M33 at Mach 0.96 [6]

Figure 9 shows the projectile at the low end of transonic flight as the majority of the projectile is subsonic and the change in profile in the tail of the projectile creates the only portion of localized supersonic flow. [6]

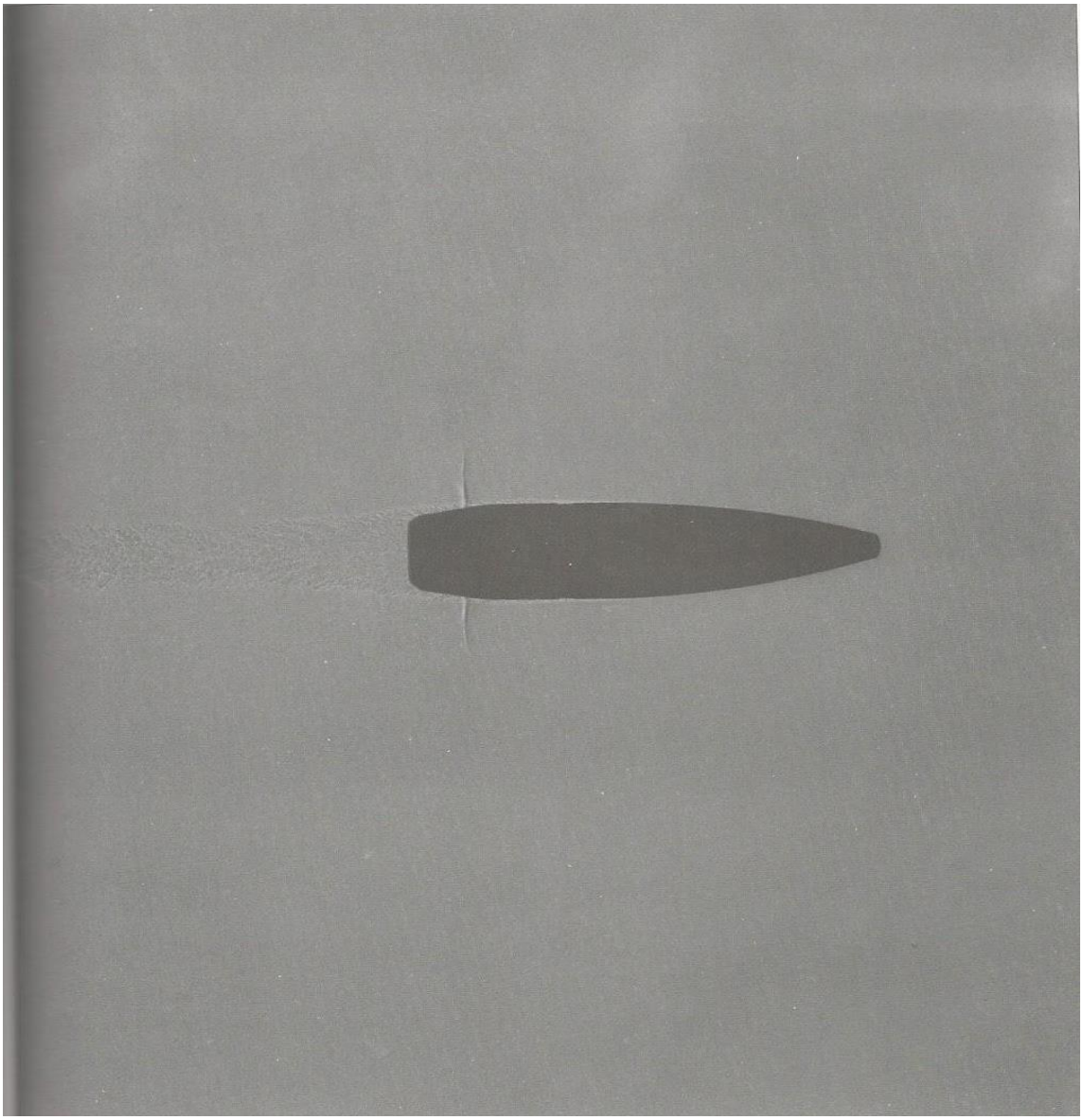

Figure 9: Field flow of caliber .50 ball M33 at Mach 0.89 [6]

The dramatic swing in drag coefficient profoundly limits the achievable accuracy in the region. The loss of achievable accuracy is the result of difficulties in predicting the exact shape of the drag curve for the given projectile, without accurate velocity data throughout the region. [4] Since the exact drag coefficient of a projectile can diverge significantly from the standard projectile in this regime (see 2.1.8 Form Factor), the accuracy of the ballistic coefficient (BC) calculation suffers greatly.

2.1.6 Subsonic Flight

The flow in Figure 10 is fully subsonic with laminar flow over the front portion of the projectile and slight turbulence in the laminar layer on the surface of the projectile. The drag coefficient is almost constant throughout this flight regime. The measured drag for the projectile in figure 10 is 0.118, for Mach numbers below 0.80. [6]

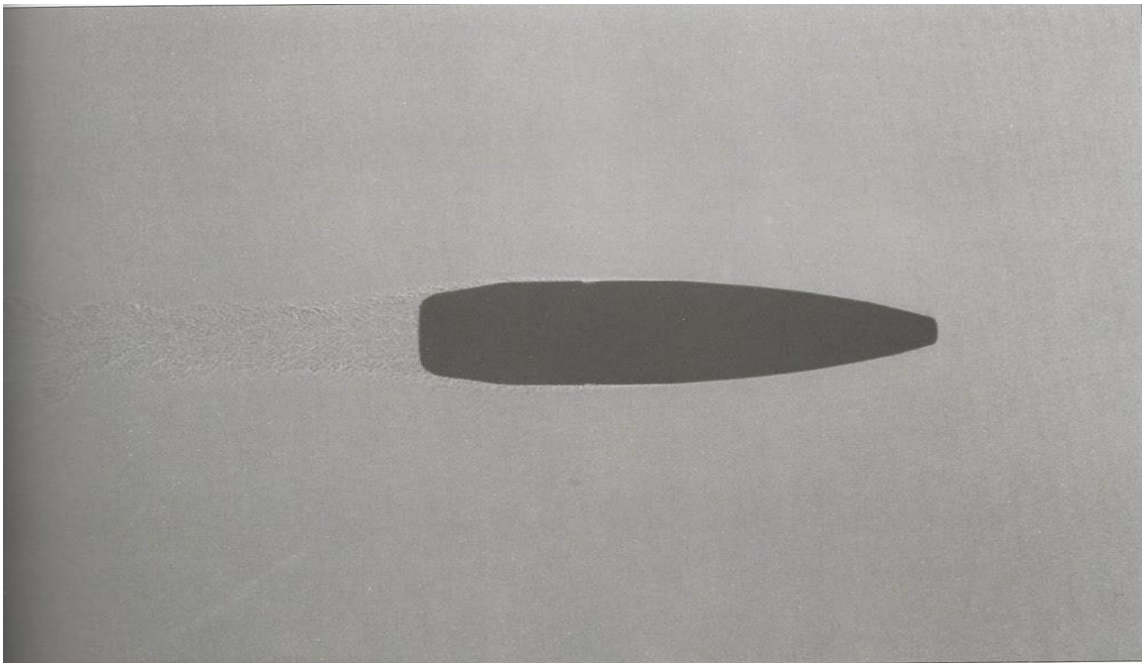

Figure 10: Field Flow of caliber .50 ball M33 at Mach 0.75 [6]

2.1.7 Ballistic Coefficient

The Ballistic Coefficient (BC) is the most widely recognized and succinct measure of a bullet's exterior ballistic performance. Knowing the BC of a bullet at a specific range allows the shooter to calculate an accurate trajectory. [4] The ballistic coefficient is a measure of how well a bullet penetrates the air. This is determined by several criteria: weight, cross-sectional area, and form factor. These factors contribute to

the whole efficiency of the projectile. Equation 1 shows how the bullet's parameters determine its BC: [6]

	$BC = \frac{W/7000}{d^2 * i} \left(\frac{lb}{in^2}\right)$	(1)

Where: BC is Ballistic Coefficient, W is the bullet weight in grains, d is the bullet diameter in inches, and i is the form factor and is non-dimensional.

To calculate the true ballistic coefficient of a projectile through testing, a minimum of two velocity measurements have to be captured during the same shot. It is important to ensure that the distance between the two velocity measurement points is precisely known and that there is at least 450 fps of velocity decay. With two known velocity measurements and a known distance, the deceleration and the average Mach number for the projectile can be calculated using Equations 2 and 3. It should be noted that a more precise measurement could be calculated by adjusting the speed of sound to correspond to the atmospheric condition at the time of firing. [6]

	$Decel. = \frac{{V_1}^2 - {V_2}^2}{2r}$	(2)

Where: V_1 is initial velocity (ft/s), V_2 is final velocity (ft/s), and r is distance between sensors (ft)

The average Mach number is calculated to allow for reference of the test projectile velocity on the same scale as the known standard projectile.

	$Average\ Mach\ \# = \frac{V_1 + V_2}{Speed\ of\ Sound * 2}$	(3)

With the experimental bullet deceleration data and the average Mach number calculated; the ballistic coefficient can be calculated from comparing the projectile's

deceleration to the deceleration of a known standard projectile, also called G projectile as described in the following section. [6]

	$$BC = \frac{Decel.\,of\ standard\ projectile}{Decel.\,of\ test\ projectile}$$	(4)

For a total flight path analysis, the velocity will need to be measured and deceleration calculated at several intervals encompassing the entire flight path.

2.1.8 Form Factor

The form factor is the result of comparing the projectile being tested against the closest standard projectile profile. This multiple is drag based, and as such, a high value means the bullet is less aerodynamically efficient than the standard projectile. [6] There are two basic standards used when comparing projectiles: The G1 and G7. These standard projectiles were developed form the work of Colonel James M. Ingalls. [3] In order to accurately calculate the drag coefficient for a projectile the form factor must be known. Figure 11 shows the effects of different form factors as drag coefficient changes for a typical long range bullet as velocity deteriorates. Note the divergence in drag in the transonic region.

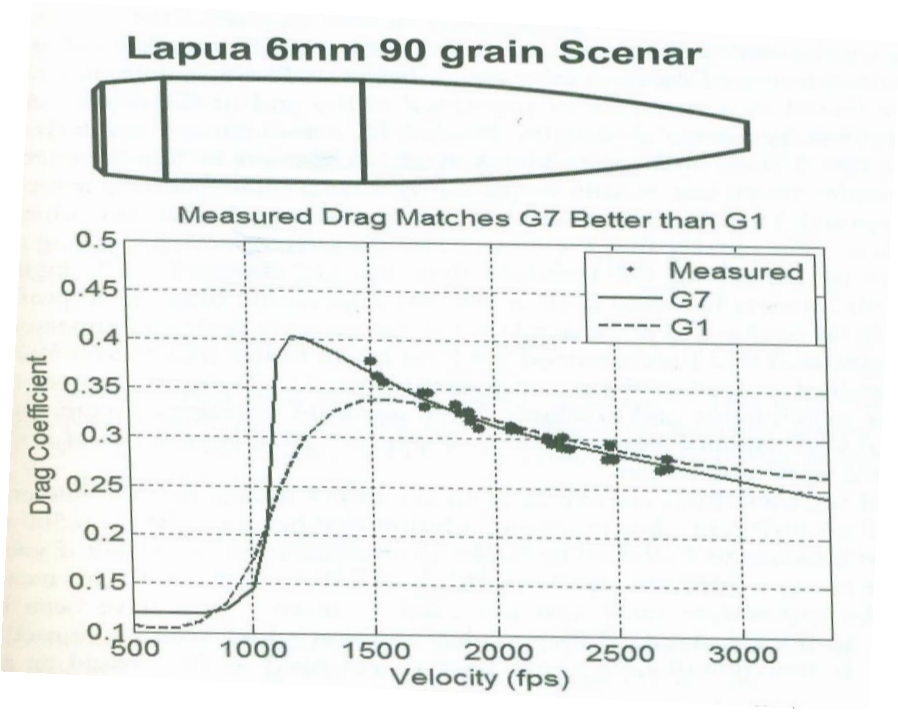

Figure 11: G7 vs G1 drag comparison [4]

The change in drag requires that velocity measurements are recorded not just at the muzzle but at several points along the flight path to be sufficiently accurate in calculating the form factor.

2.2 Velocity and Trajectory Capturing Methods

2.2.1 Optical Sensors

Currently the most prolific method for determining the muzzle velocity of a revolving projectile is the employment of optical sensor chronographs. These devices use a pair of light detecting optical sensors that react to the shadow of a bullet as it passes through the optical window. The time difference between the first sensor and the second being triggered determines the velocity. While these sensors are economical they have several drawbacks. As seen in figure 12 the apparatus requires the user to place the instrument in close proximity to the muzzle (10-12ft) and shoot through the indicated

detection window. When employed at extended ranges (300+ yards) replacement of electronics can become a recurring operational expense if the users aim is not precise. [1]

Figure 12: Optical chronograph [14]

The reliance on background lighting is another limitation. Inconsistencies due to changes in outdoor lighting conditions can greatly decrease the precision of these instruments, sometimes causing them to return error messages. [1]

This method is also popular for calculating BC. By shooting over two chronographs placed a known distance away from each other the decay in velocity between the two points can be used to accurately calculate the true ballistic coefficient of the projectile. The biggest problem with this method is practicality. Error analysis reveals that the chronograph should be placed as far apart as possible (300+ yds.). If the chronograph is only accurate to +/- 5 fps the distance is needed to ensure adequate velocity decay (450+ fps). Increasing the distance between the two chronographs reduces the error, but increases the likelihood of striking the downrange chronograph with an errant projectile. [4]

2.2.2 Acoustic Sensors

Acoustic sensors are used to detect the audible crack of the bullets supersonic passage to determine projectile velocities. The sensors do not need to be placed in line with the projectile path and risk being struck by the projectile. The range at which these sensors can detect the bullets passing is greatly increased over optical sensors. The range at which the acoustic sensors are placed downrange must be known with a high degree of accuracy to ensure that the standard of +/- 1% error in measured BC is maintained. [4] Acoustic sensors that are capable of 0.5 ms time resolution and the audio processing equipment that accompanies them are cost prohibitive for the avid enthusiast and are useless for observing the transonic or subsonic flight regimes due to the absence of supersonic audio signal. [4] Acoustic sensors have been developed and deployed for the detection and location of hostile shooters by the U.S. Military. [5]

2.2.3 Doppler Radar

Doppler radar is the most accurate system used to perform flight path analysis of revolving projectiles. Using a directional radar unit, projectiles are fired and tracked for very long distances. With proper calibration trajectories can be recorded down to the foot. From these trajectories accurate and precise drag data can be obtained. [4] This technology has been used successfully by the US Army Ballistics research lab and NASA to look at all regimes of projectile flight. [12] The major drawback to this level of technology is the expense and exclusiveness. The use of Laser Doppler velocimeters is strictly controlled by the US government. [2] The technology has been recently used by Lockheed Martin to look at wind deflection across the whole flight envelope. [4]

2.3 Electric Field Sensors

2.3.1 Background

Over the years, numerous techniques for electric charge/electric field/voltage detection and measurements have been developed. Electric field sensors were utilized in projectile detection as early as 1960s by Nanevicz and Wasdsworth. [7] They used a shielded metal tube as an induction sensor and projectiles passing through the tube produced a recordable electric potential. Later work involved use of large, electrically isolated plates, on which the signal was induced and detected [12, 13]. A revolving projectile while leaving the rifle's muzzle and interacting with air media acquires an electric charge ranging from 10^{-8} to 10^{-12} C, this charge produces an electric field, which can be sensed and measured. [9] Electric field sensing of projectiles has not received much attention until recently, when new generations of smaller, low power sensors were developed. [9]

2.3.2 The Employed Sensors

A technique for electric field sensing was invented based off an RF amplitude-modulated varactor sensing circuit. [8, 10] A typical electric field pulse created by a revolving projectile requires the sensor to operate in a 2-5 kHz frequency range. A group of such sensors arranged into an array with known distances between them have been proven to detect and, through triangulation, report the direction of the moving projectile. A successful field test of the first generation sensor shown in figure 13 has been conducted by Dr. Noras in conjunction with the Army Research Laboratories at the Aberdeen Proving Grounds in Maryland. [9]

Figure 13: First generation sensor

Figure 14 shows the electrostatic field disruption of the passing projectile as captured by the sensor array.

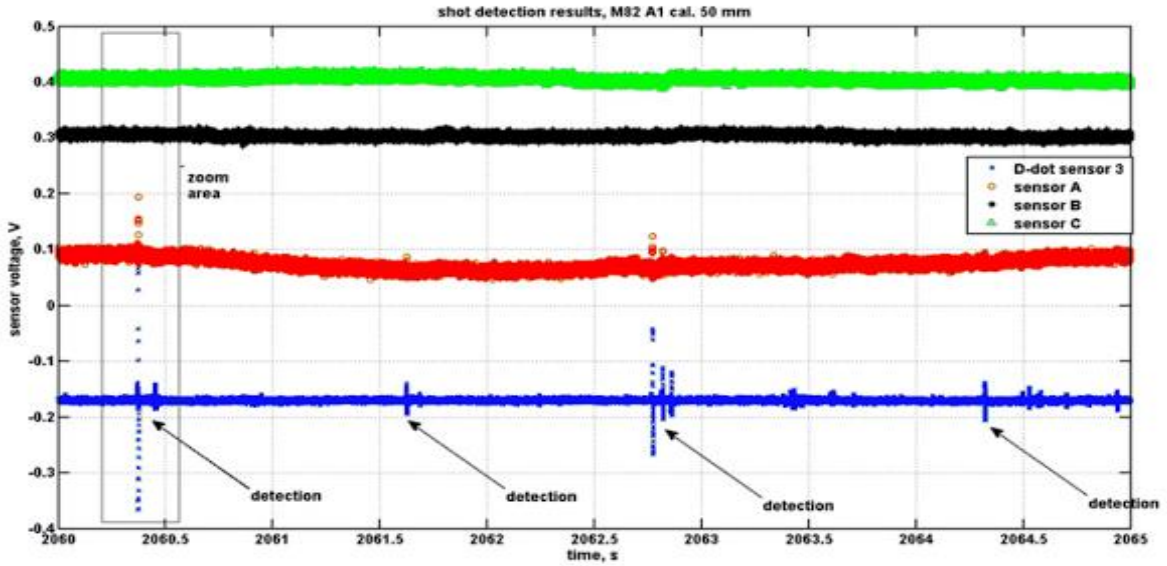

Figure 14: Detection spikes of a passing projectile [9]

Figure 15 displays the primary sensor version used in the research.

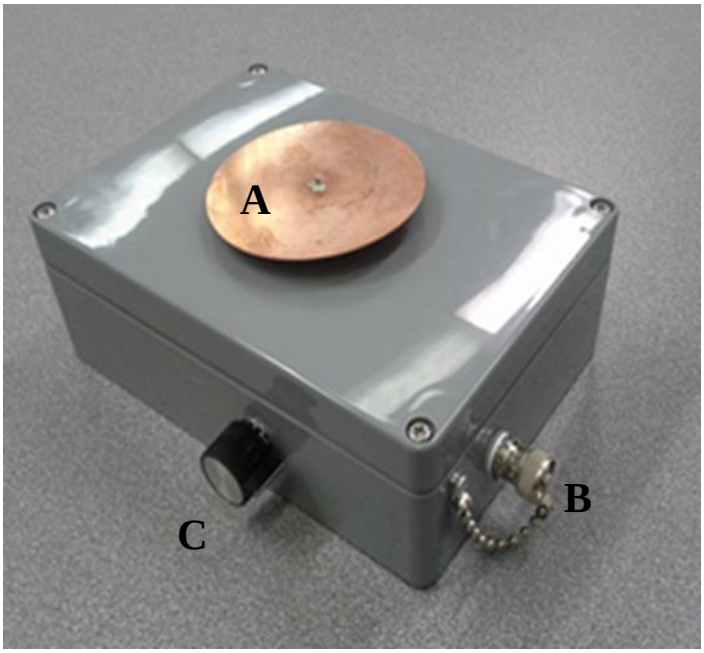

Figure 15: Electric field sensor

Where: A denotes the sensor plate, B denotes the analog output, C denotes the gain adjustment

The development of this type of sensor has many advantages for capturing time based data on revolving projectiles. Electric field sensors are not constrained to the supersonic flight regime like acoustic sensors. They do not require the projectiles to pass within close proximity as optical sensors. Multiple electric field sensors can be deployed simultaneously through the entire flight path at a substantial cost savings over using Laser Doppler velocimeters and once further developed should be capable of the same data resolution.

CHAPTER 3: RESEARCH METHODOLOGY

3.1 Introduction

Testing started with laboratory analysis and development of data collection methods using low velocity projectiles and validation using high velocity test sessions. Improvements were implemented from each test and this cycle was repeated as new hypotheses and testing methods were evaluated.

3.2 Laboratory Feasibility Testing

3.2.1 Objectives

The objective of laboratory feasibility testing was to validate the system used to capture and record data and to verify detections and velocity calculations in a laboratory setting with low velocity projectiles. While individual sensors had previously been utilized to detect the presence of a passing bullet, they had not been used in pairs for determining a time differential between the signals.

3.2.2 Setup

Sensors were placed in a linear array approximately 1 foot apart, BNC to alligator connectors were used on the analog outputs and connected to an analog data acquisition device. A National Instruments USB-6009 DAQ was employed in the early testing stages. The USB-6009 DAQ USB output was connected to a computer running National Instruments LabVIEW software containing a virtual instrument (VI) that was developed to capture the peak voltage outputs from the sensors and to save them to a file for later

evaluation. A screen shot of the VI is visible in APPENDIX A. A low velocity projectile was fired over the array for these indoor laboratory tests.

3.2.2 Equipment

The key pieces of equipment for these initial laboratory feasibility experiments are noted in Table 1:

Table 1. Laboratory feasibility equipment

Item	Qty	Use
Electric Field Sensors	2	Detect the disturbance in the electric field from the bullets passage
Dell Laptop	1	Running the LabVIEW VI and saving the data
National Instruments USB 6009 DAQ	1	Data Acquisition Device used to collect the analog voltage readings
Nerf Dart Gun	1	Used to fire low velocity foam darts over the sensors in the lab, producing a change in the electric field
Wooden Ballista	1	Used to fire low velocity plastic or metal slugs over sensors in the lab, producing a change in the electric field

3.2.3 Deliverables

The session was used to verify the proper function of the data collection system and ensuring the sensors were functioning and positively detecting passing projectiles in a controlled laboratory environment.

3.3 Field Feasibility Testing

3.3.1 Objectives

The objective of this portion of testing was to expand on successes in the lab and to validate the detection and velocity calculation of supersonic projectiles in a field environment. The goal for accuracy being set at +/- 1% of the referenced velocity.

3.3.2 Setup

Two sensors were placed in a linear array a measured 5 feet apart. BNC to alligator connectors were used on the analog outputs and connected to a USB 6009 DAQ or a MYDAQ. The DAQ USB output was connected to a computer running LABVIEW software containing a VI created by the author that captures the peak voltage waveform outputs from the sensors and saves them to a file for evaluation. An optical chronograph was placed directly in front of the first sensor and directly behind the second sensor. The two optical chronographs are used for velocity validation of the sensor array. A rifle firing .277 in (6.8 mm) supersonic projectiles was fired over the sensors. The first chronograph was placed a measured 10 ft from the muzzle of the rifle. The process of firing and recording data was repeated on four separate dates.

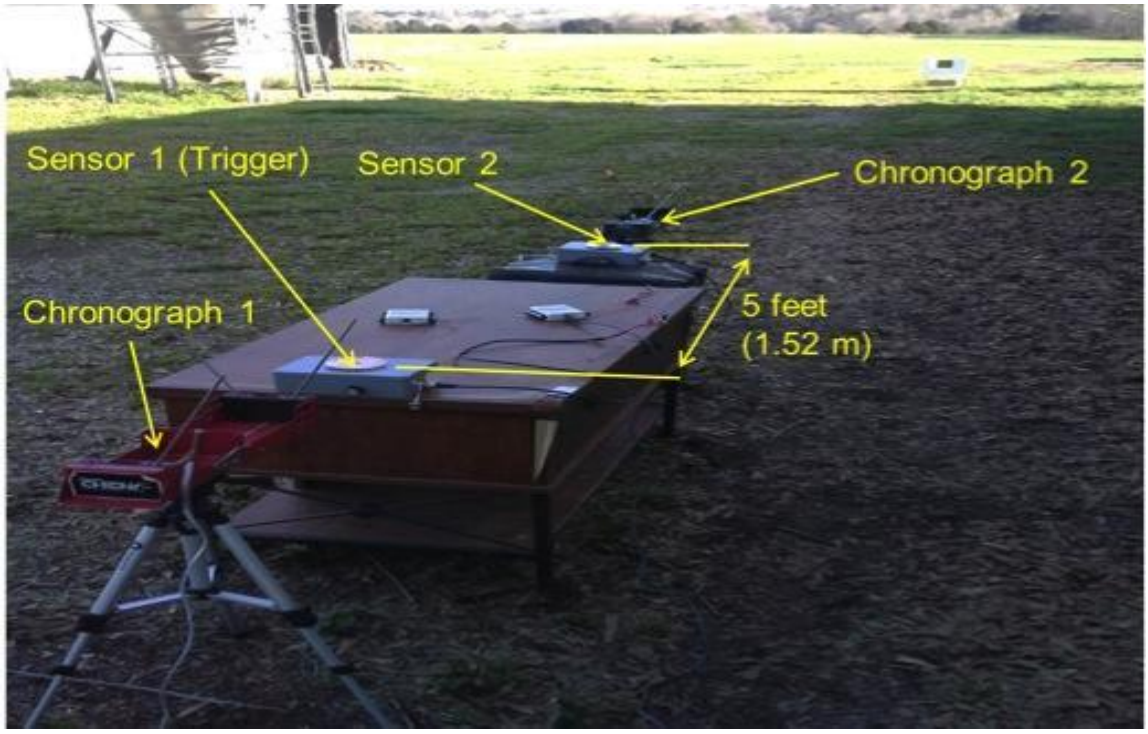

Figure 16: Field test setup

3.3.2 Equipment

Table 2. Field feasibility equipment

Item	Qty	Use
Electric Field Sensors	2	Detect the disturbance in the electric field from the bullets passage
Dell Laptop	1	Running the LabVIEW VI and saving the data
National Instruments USB 6009 DAQ	1	Data Acquisition Device used to collect the analog voltage readings
Chronographs	2	Capturing of reference velocities
Rifle	1	AR-15 6.8 SPC caliber
Ammunition	N/A	Handloaded 110gr Match ammunition

The weapon system used for all high velocity testing is an AR-15 variant chambered for an intermediate caliber of 6.8mm (.277 dia.) The weapon has a history of accuracy and consistency, reliably produced 3 shot groups on the order of .25 to .50 inch from a distance of 100 yards. The author is the sole owner and has fired the weapon in excess of 300 times. The weapon is pictured in Figure 17.

Figure 17: Test rifle

Figure 18 shows an example of the accuracy potential of the weapon system.

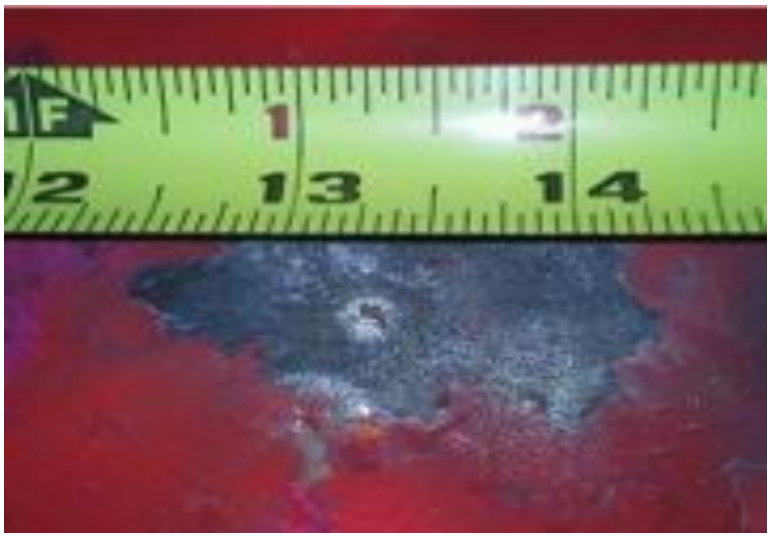

Figure 18: 4 shots at 305 yards

Ammunition for all high velocity testing was hand loaded by the author to ensure the highest consistency and lowest standard deviation possible. The powder charges are measured to +/- 0.1 grain and the projectile used is a 110 grain match grade bullet. The ammunition averages 2600 feet per second based on optical chronograph measurements.

Figure 19: 6.8 SPC II ammunition

3.3.3 Deliverables

The session was used to validate the sensors ability to capture peaks from supersonic projectiles and calculate velocity readings from the captured peaks. The session also served to establish the procedures used in sensor setup and tuning for peak detection and velocity analysis. The sensor's velocity resolution accuracy was tested against commercially available chronographs.

3.4 Laboratory Refinement Testing

3.4.1 Objectives

This portion of testing was used to test possible hypothesis for improving detection consistency and accuracy.

3.4.2 Setup

The two sensors used in prior test were recalibrated to provide a baseline at which to begin evaluations. This process entails placing the sensors individually in a created electromagnetic field and observing the output from the sensors. The sensor frequency range and sensitivity were adjusted until the detected signal mirrored that of the created electromagnetic field.

Low velocity projectiles were then fired over the sensors and detailed notes on the consistency and output of both sensors used for testing were recorded. Several hypothesis and test specifically directed at determining the cause of inconsistencies were conducted. The tests were conducted over a series of several sessions.

3.4.3 Equipment

Table 3: Laboratory refinement Equipment

Item	Qty	Use
Electric Field Sensors	2	Detect the disturbance in the electric field from the bullets passage
Oscilloscope	1	Capturing sensor peaks and saving the data
Grounding wire	1	Grounding of oscilloscope
Wooden Ballista	1	Used to fire low velocity plastic or metal slugs over sensors in the lab, producing a change in the electric field
Dense foam slugs	N/A	Low velocity projectiles

3.4.4 Deliverables

The section served to develop and document methods for producing consistent detection in a laboratory environment and for developing testing procedures with high velocity projectiles. Evaluation of the accuracy potential of the electric field sensor in comparison with referenced velocities.

3.5 Field Refinement Testing

3.5.1 Objectives

The purpose of this section was to field test the proposed methods of enhancing detection that provided promise during the laboratory refinement testing.

3.5.2 Setup

The sensors were placed in a linear array with a measured 5ft between the sensor plates. The test apparatus also included a target with graduated markings placed behind the last sensor. This was used to verify the height of the projectile above the sensor plate. An optical chronograph was placed in front of the lead sensor to record reference velocities. This chronograph was placed a measured 10ft from the muzzle of the weapon. The sensors were grounded using the paperclip method as previously tested in low velocity refinement test. Grounding was repeated prior to each shot. An oscilloscope was used to capture the sensor detection peaks and save the captured waveforms for further analysis. Figure 20 shows the final high velocity testing setup. Employing a piece of extruded aluminum and adhering the sensors with hook and loop tape ensured the plate centerline distance remained constant at 5 ft. The aluminum also allowed the team to ensure that the sensors were perfectly level in the horizontal plane to further enhance the accuracy of the detections.

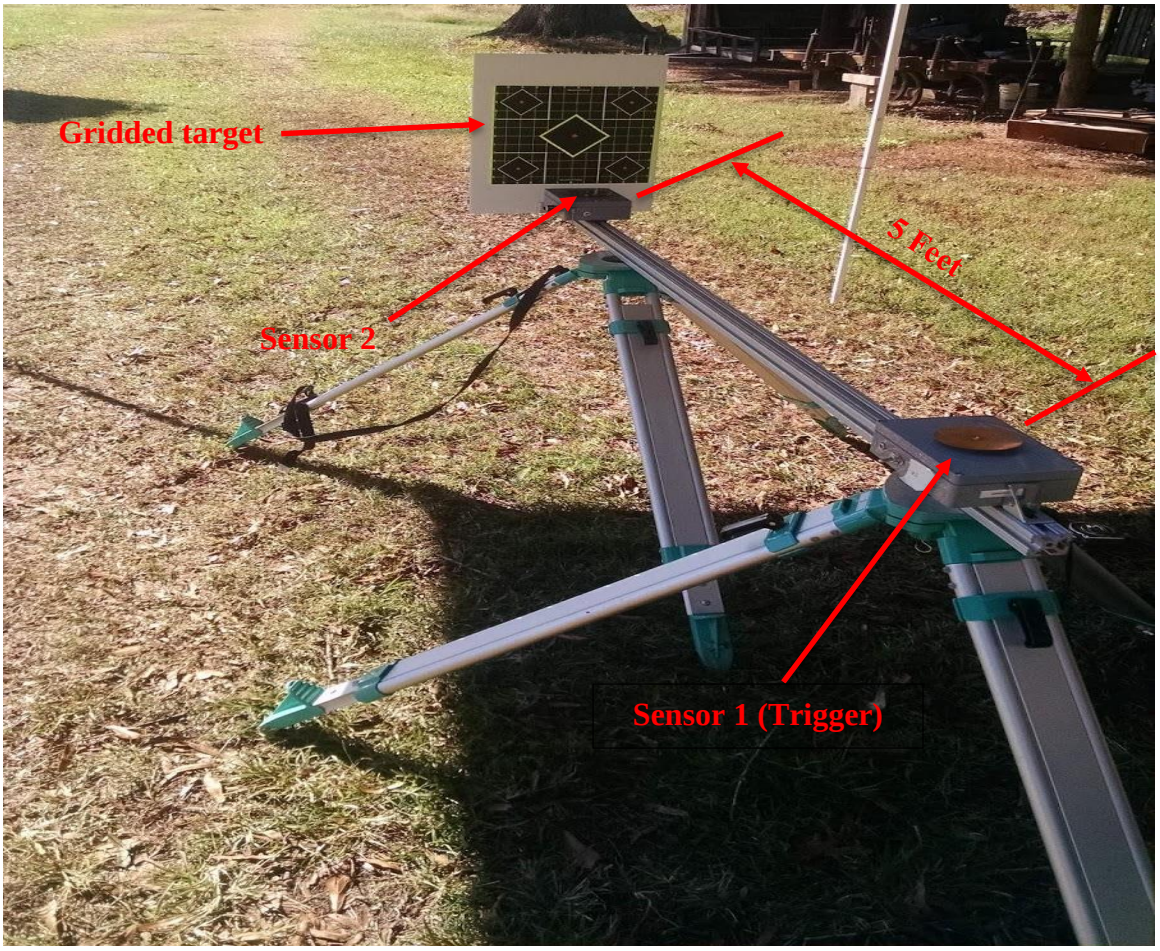

Figure 20: Final high velocity test setup

Two range sessions were scheduled for this portion of testing. The first being performed at an indoor range facility. This test ensured that atmospheric interference would not affect sensor detection. The second test took place at the outdoor location previously used in all other phases of testing.

3.5.3 Equipment

Table 4: Field refinement equipment

Item	Qty	Use
Electric Field Sensors	2	Detect the disturbance in the electric field from the bullets passage
Oscilloscope	1	Capturing sensor detections and saving the data
Chronographs	1	Used to compare sensor accuracy
Rifle	1	AR-15 6.8 SPC caliber
Ammunition	N/A	Handloaded 110gr Match ammunition
Sensor Grounding Clips	2	Grounding of senor plates prior to firing

3.5.4 Deliverables

The section was used to validate testing procedures developed in the laboratory refinement section, and the accuracy of sensor detections versus commercially available chronographs.

3.6 Indoor Sensor Analysis and low Velocity Testing

3.6.1 Objectives

A thorough analysis of the prior and current generation sensors was conducted to characterize any differences between the 2 generations of sensors being used and to test several hypnotists that had arisen from the prior tests.

3.6.2 Setup

The sensors were not adjusted from the prior test and were placed individually on a test bench and connected by a BNC cable to the same oscilloscope used in the previous

test. The wooden ballista was used to fire low velocity projectiles over the sensors. Any detected peaks were saved for analysis. The same procedures were used to test the prior generation sensor.

3.6.3 Equipment

Table 5: Indoor sensor analysis equipment

Item	Qty	Use
Electric Field Sensors	2	Detect the disturbance in the electric field from the bullets passage
Oscilloscope	1	Capturing sensor peaks and saving the data
Grounding wire	1	Grounding of oscilloscope
Wooden Ballista	1	Used to fire low velocity plastic or metal slugs over sensors in the lab, producing a change in the electric field
Dense foam slugs	N/A	Low velocity projectiles

3.6.4 Deliverables

The session served to test and characterize sensor detection issues and document level of sensor issue occurrence and successful detections for both generations of sensor.

CHAPTER 4: RESULTS

4.1 Laboratory Feasibility Results

The low velocity testing showed that detection and velocity calculation were possible and displayed promise that the data acquisition – sensor system would detect a supersonic projectile. Figure 21 is a sample of the positive detection from early low velocity testing.

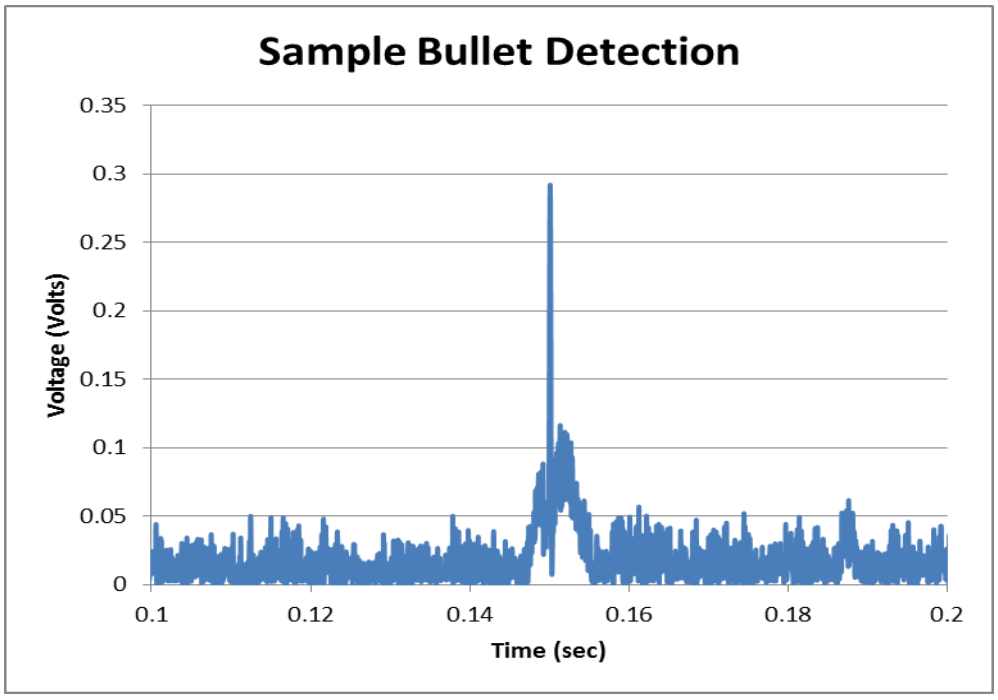

Figure 21: Single sensor peak detection at 20 kSamples/s

Figure 22 shows low velocity voltage peak detections used to calculate the projectiles velocity.

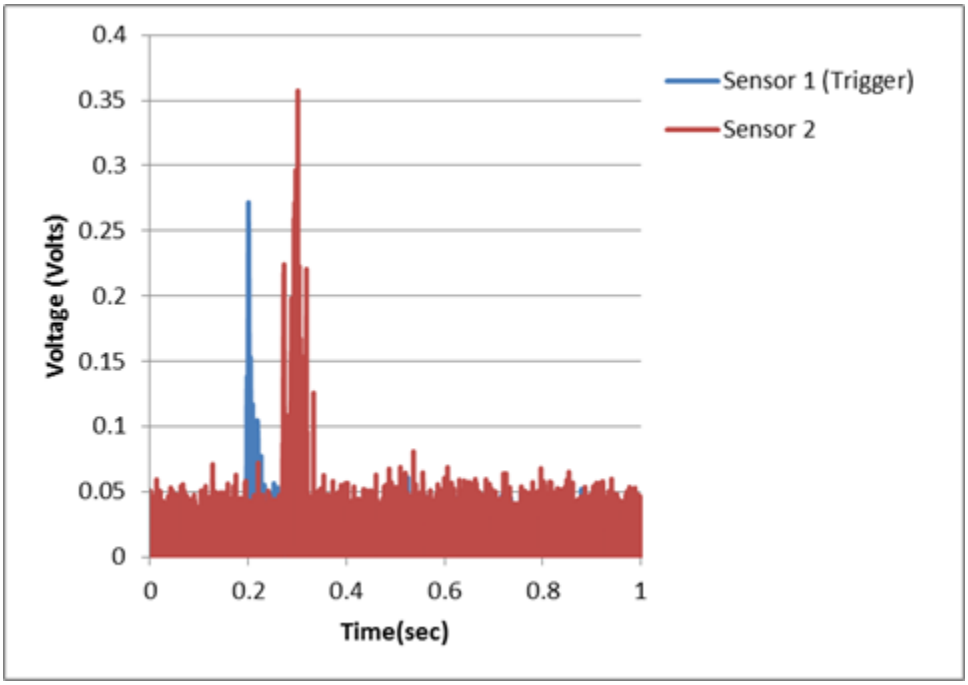

Figure 22: Low velocity projectile peak detection at 20 kSamples/s

Average velocity measurements for the low velocity projectiles varied between 10 – 30 fps. Testing at this stage was conducted using a USB 6009 DAQ and a sample rate of 20 kSamples/s. Both sensors were capable of consistent positive detection.

4.2 Field Feasibility Results

The test proved successful at producing velocity readings of supersonic projectiles that were consistent with those recorded by the chronographs. Figure 23 is a graph of the raw sensor peaks detected and used for velocity calculations. The raw data was uploaded to MATLAB where a peak finding function was employed to return the peak locations based on data point reference. Knowledge of the resolution rate and counting the steps between detection peaks delivered the time elapsed between detections. The MATLAB code used for analysis can be seen in APPENDIX C. The basic equation for velocity calculations is shown in Equation 5.

	$Velocity = \frac{D}{\Delta t} \ (\frac{ft}{sec})$	(5)

Where: D is the measured distance between the sensors, and Δt is the time elapsed between detection peaks.

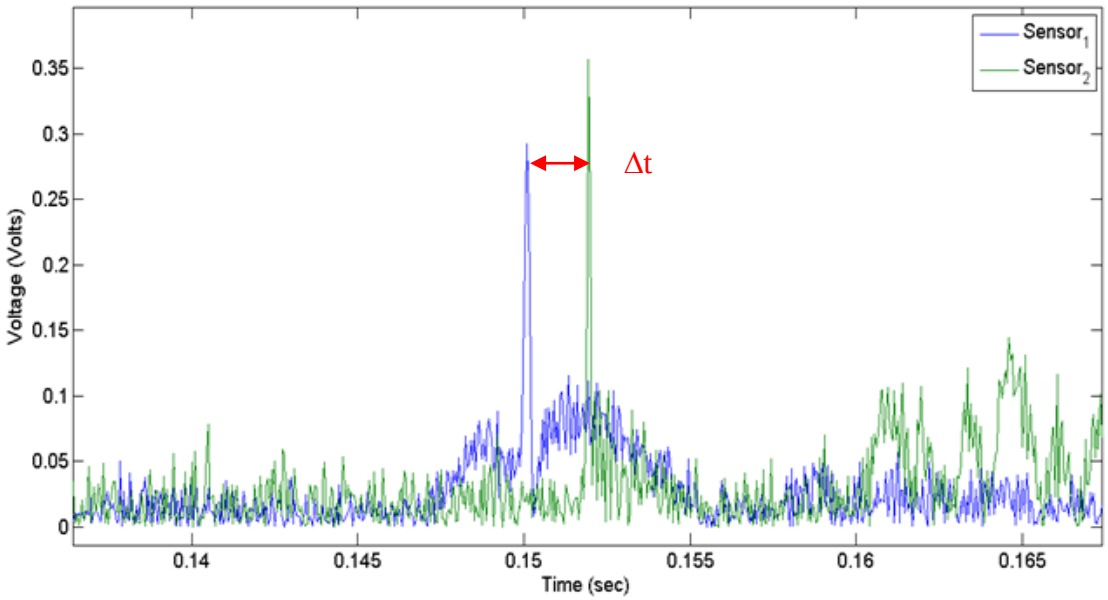

Figure 23: Sensor peak velocity detection

The time delay between the leading (sensor 1) peak and trailing (sensor 2) peak ranged from 1.85 ms to 2.00 ms. Figure 24 shows the calculated sensor muzzle velocity readings and the comparative velocities recorded from the chronographs.

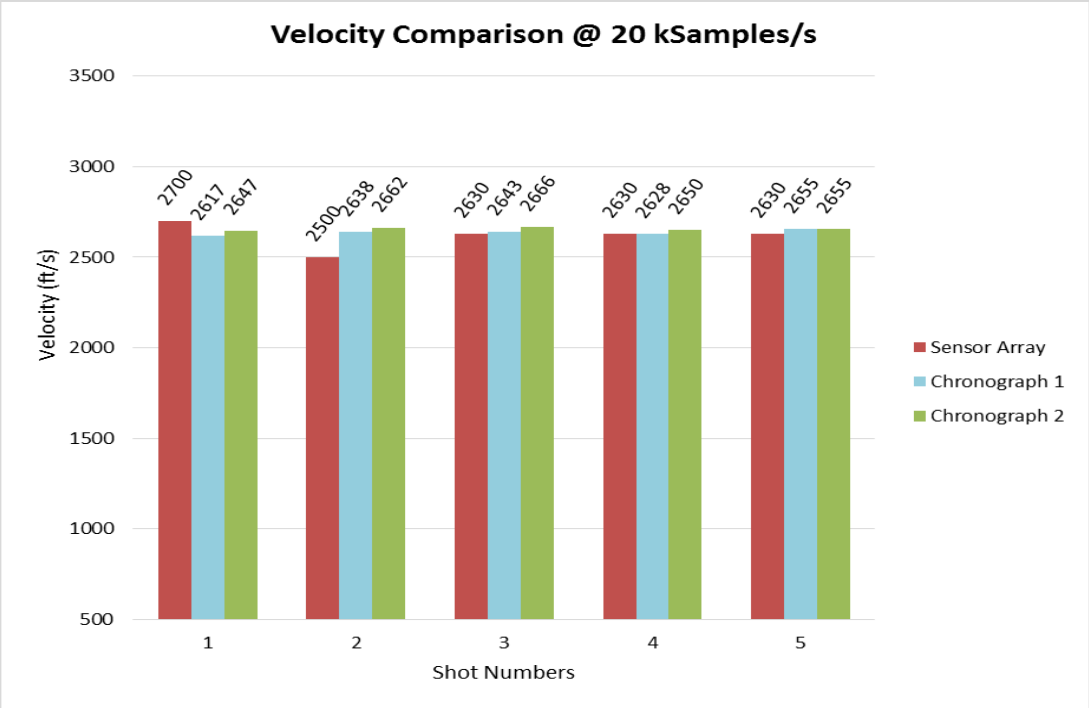

Figure 24: Velocity comparison 20 kSamples/s

Figure 25 displays the percent difference values created by comparing the average velocity measurements of the chronograph with those of the sensor array shown in figure 24. The average percent difference for this stage of testing was 2.09%. Equation 6 was used to calculate the percent difference.

	$Percent\ Difference = \frac{(V_{avg} - V_s)}{(V_{avg})} * 100$	(6)

Where: V_{avg} is the averaged velocity from the chronograph measurements and V_s is the velocity measured form the sensors

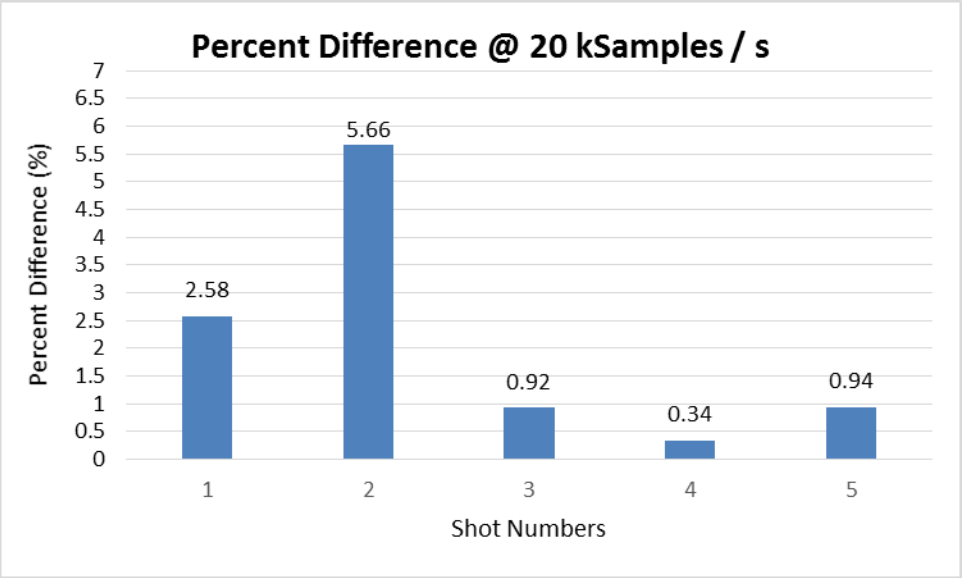

Figure 25: Percent difference for 20 kSamples/s

4.2.1 Data Collection Resolution Analysis

The first portion of field testing was conducted collecting data at 20k samples per second. This sample rate was found to be insufficient for providing a true velocity reading. Considering that a 20 kSamples/s rate produces discrete 0.05 ms time steps, implies that for the 0.4 ms duration of a projectile detection spike, only 8 data points were collected. From the analysis it was found that when sampling at 20 kSamples/s and firing projectiles traveling at approximately 2500 fps the data collection had a zero error velocity resolutions of +/- 60 fps between sampling steps. Increasing sampling to 200 kSamples/s reduces this to +/- 6 fps. Figure 26 is a graphical representation of this analysis.

Based on this observation subsequent velocity testing would employ a LabVIEW MYDAQ data acquisition system sampling at 200 kSamples/s.

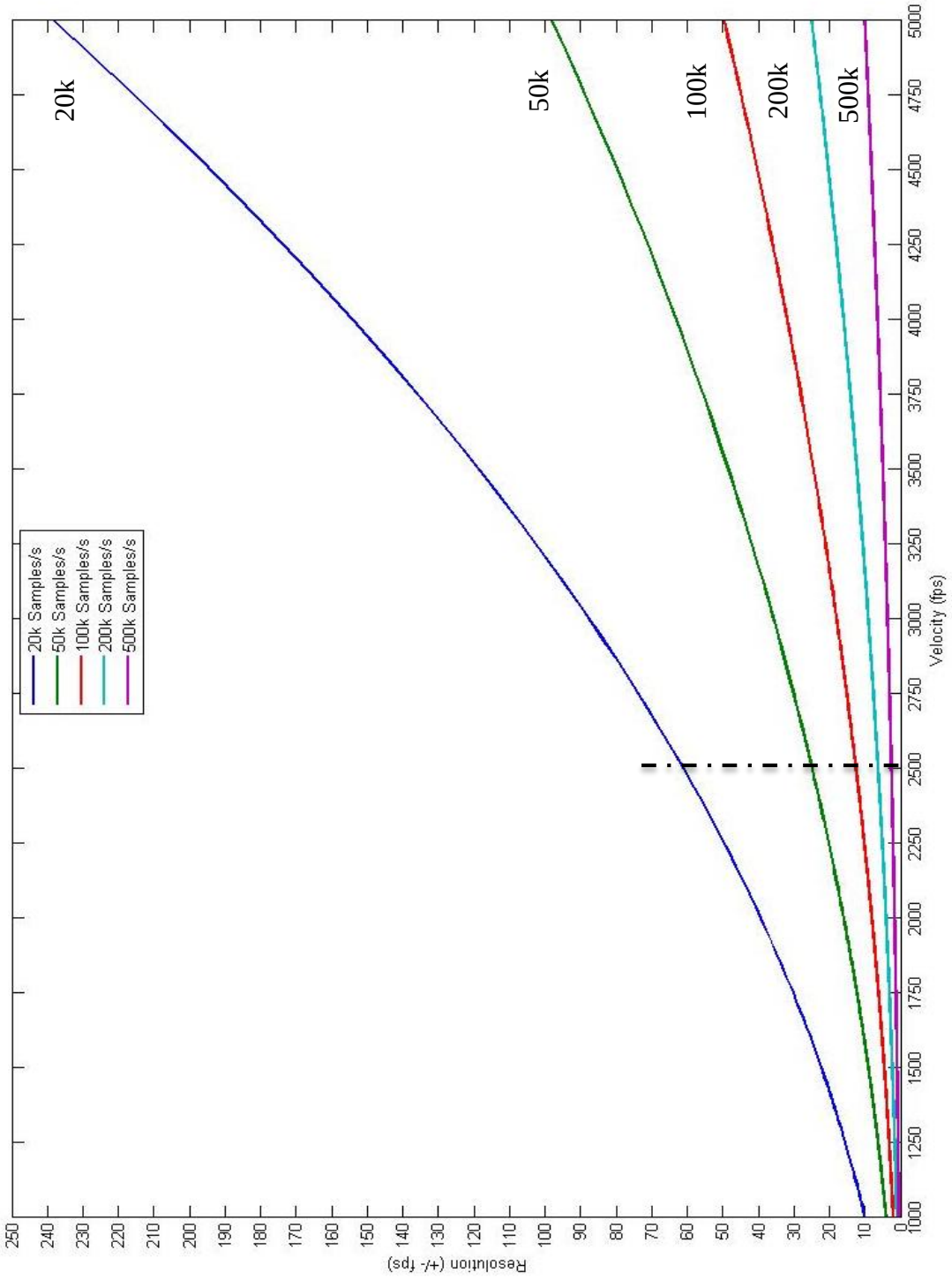

Figure 26: Sensor resolution analysis

Careful consideration of other errors associated with the data collection process was also analyzed. The accurate measurement of distance between the two sensor plates was critical in ensuring the reduction in velocity measurement error. A second analysis was conducted to combine the data collection and measurement error. Measurement error was established at 0.0625 inch for the test given the use of a standard construction tape graduate at 1/32 inch. The resolution error was allowed to vary with the sample collection rate. Equation 7 and 8 were employed to create the graph shown in figure 27. The MATLAB code is visible in APPENDIX B.

	$$Vmax = \frac{D + \Delta d}{\Delta t - (2\ E)}$$	(7)

Where: Vmax is the maximum velocity with error, D is the distance between sensor plates, Δd is the error in sensor distance measurement, Δt is the time between sensor detections, E is the error in data collection resolution and varies with sampling rate.

	$$Vmin = \frac{D - \Delta d}{\Delta t + (2\ E)}$$	(8)

Where: Vmin is the minimum velocity with error, D is the distance between sensor plates, Δd is the error in sensor distance measurement, Δt is the time between sensor detections, E is the error in data collection resolution and varies with sampling rate.

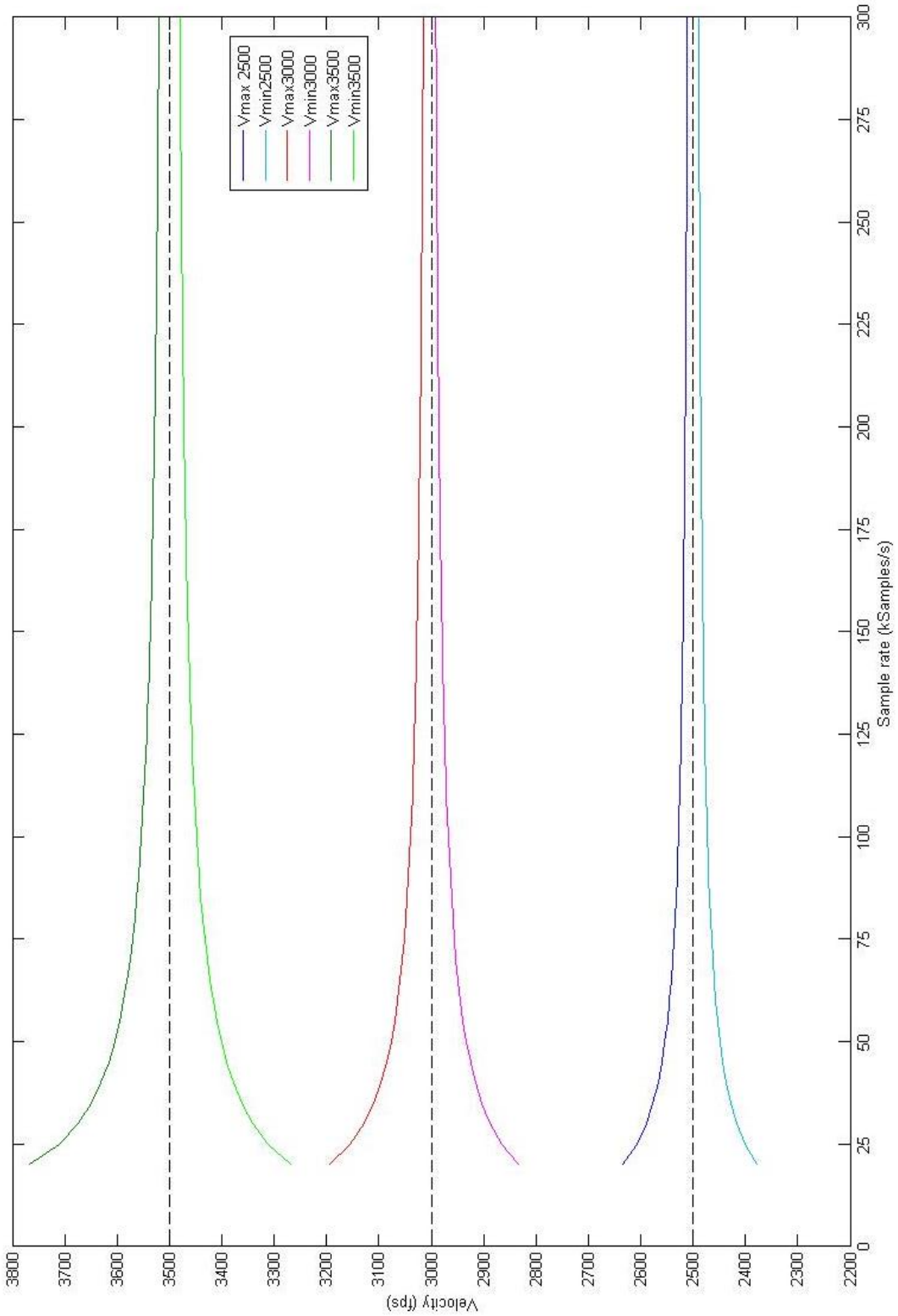

Figure 27: Velocity error analysis

The analysis shown in figure 27 strengthens the conclusion that higher sampling rates are necessary for achieving the desired velocity measurement accuracy of +/- 1%. A second set of tests were conducted using the increased sampling rate of 200 kSamples/s. Figure 28 displays the velocity comparison for the second round of test.

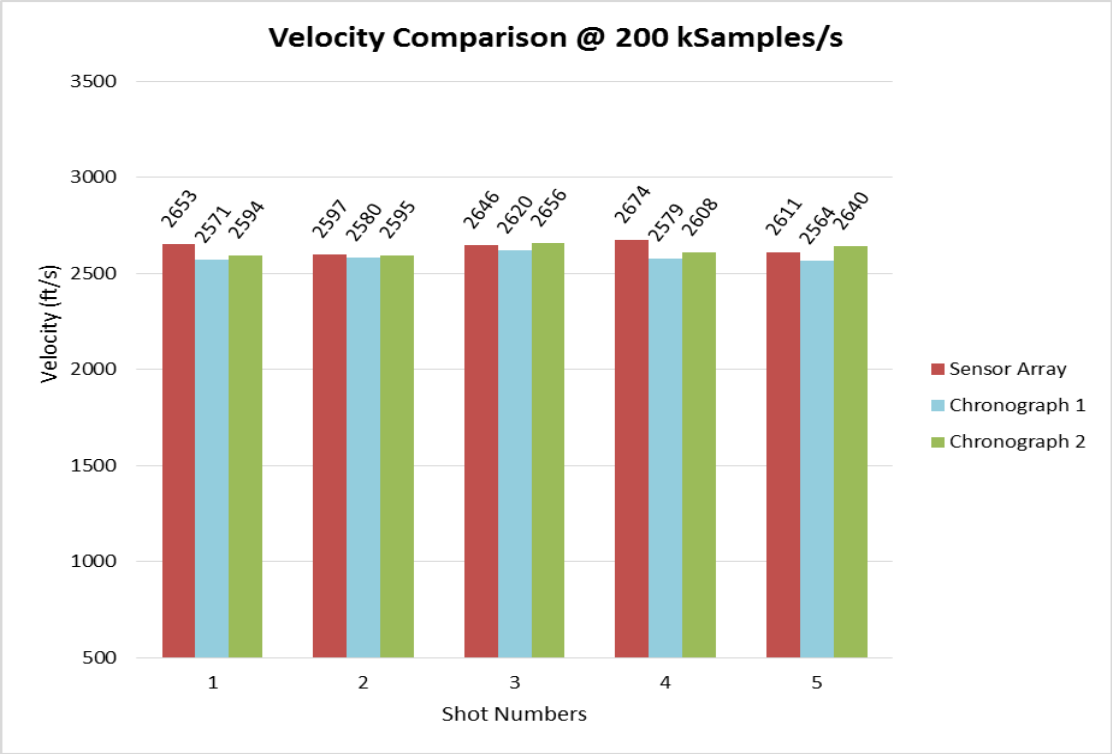

Figure 28: Velocity comparison 200 kSamples/s

This round of testing produced velocities with a reduced average percent difference of 1.36%, that approached the +/- 1% goal of the test. Figure 28 displays the sensor array velocity measurement percent difference from the referenced chronograph velocity measurements in figure 28. The increased percent difference in shots 1 and 4 are credited to increased sensor noise level that made detection of the true peaks difficult.

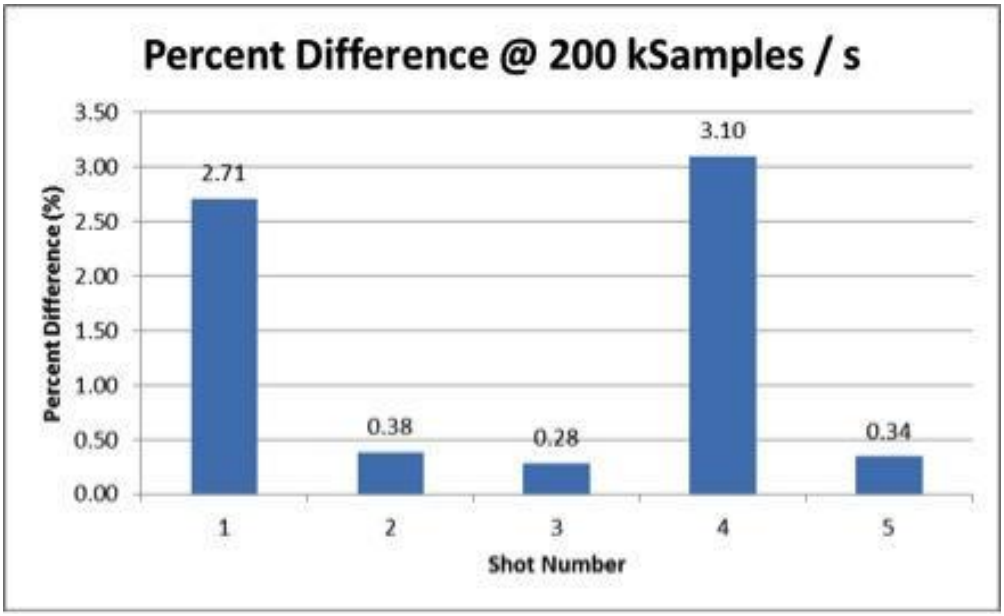

Figure 29: Percent difference results 200 kSamples

Issues arose over several field testing sessions. Consistent detection of passing projectiles proved difficult under field conditions. The sensor started to experience an increased noise level and a reduction in sensitivity. Initially the sensors displayed a signal noise level ranging from (0.03 - 0.04 Volts). The noise level continued to increase to (0.06 – 0.10 Volts). The increased noise level made it difficult to determine the exact peak to use in velocity calculations. Figure 29 is an example of a projectile detection that due to noise and reduced sensitivity, could not produce an accurate velocity reading.

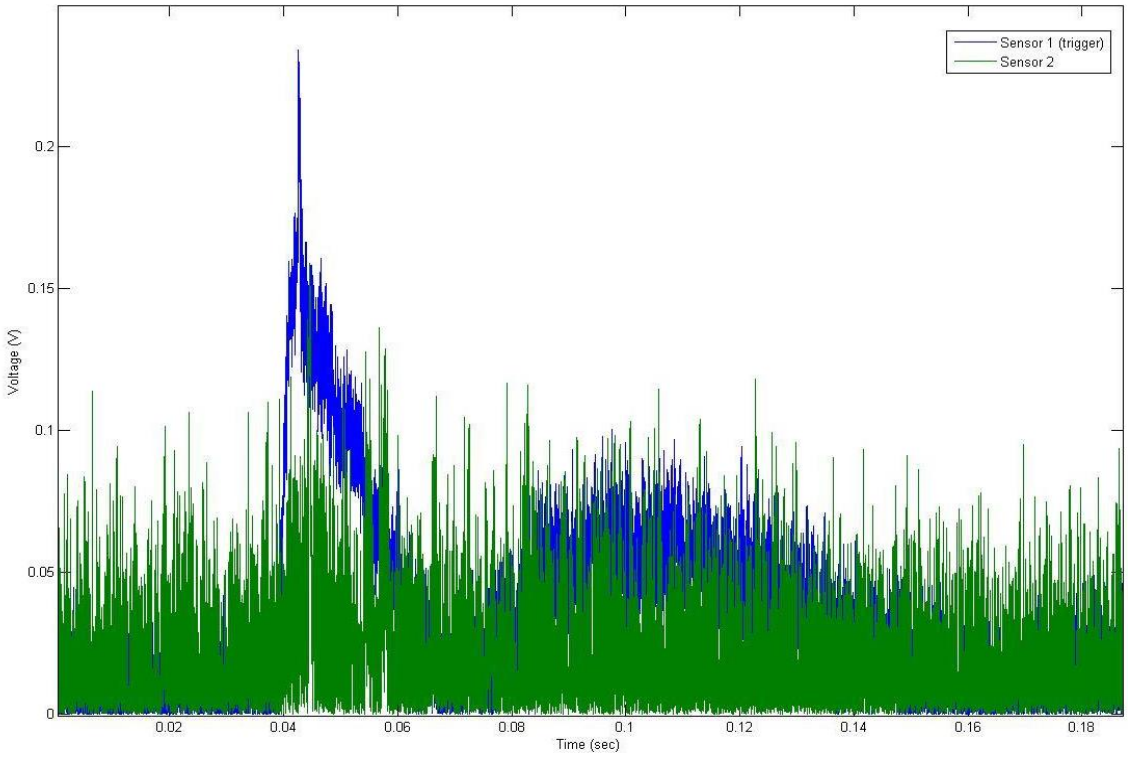

Figure 30: Sensor noise from increased sampling rate

Where in earlier testing it was possible to get positive peaks from projectiles passing approximately 12 inch above the sensor plates the team struggled to collect detections with the projectiles passing 4 inches from the plate surface. Peak detection voltages decreased in accordance with the decrease in sensitivity. Initial positive detections produced output voltages ranging from (2.0 – 1.5 Volts) as seen in figure 31. Later positive detections produced output voltages of only (0.30 – 0.15 Volts) as seen in figure 30. Refinements to the data collection methods improved the sensor resolution, however the increase in sensor noise level and the reduction in sensor detection sensitivity made it impossible to collect further samples.

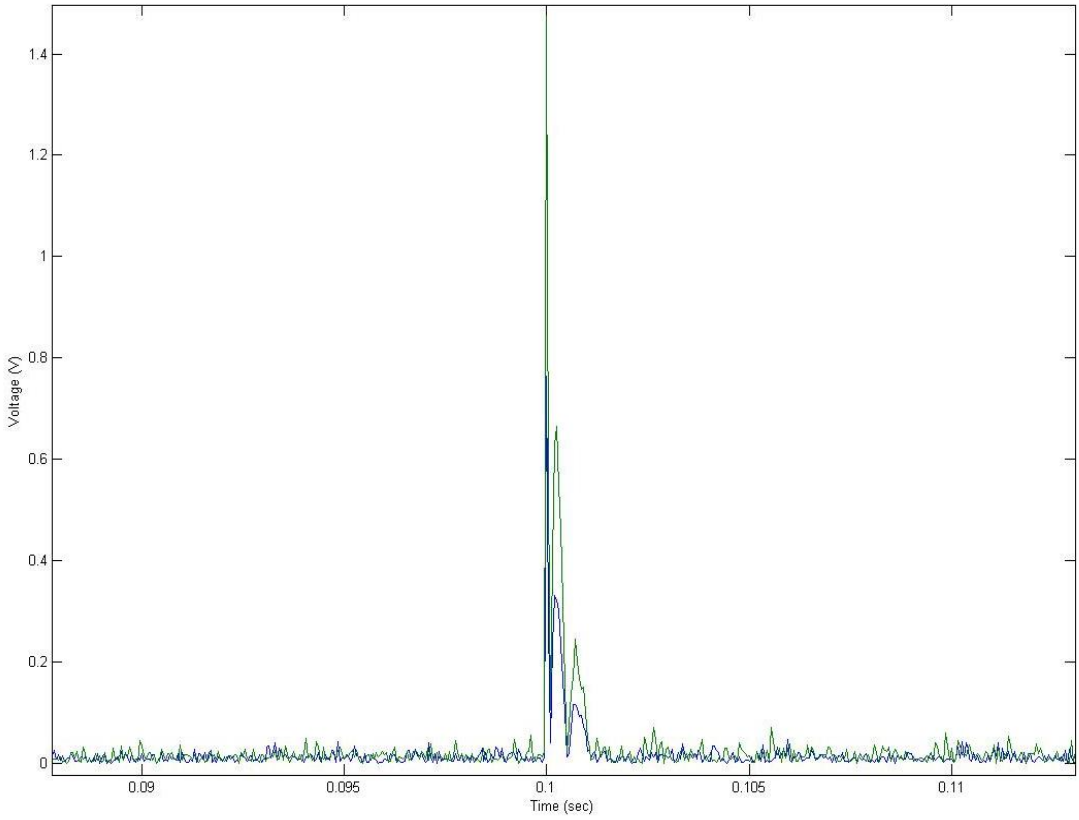

Figure 31: Initial high velocity test detection

4.3 Laboratory Refinement Results

During calibration it was observed that when the sensor detection plate was grounded by touching the plate with a fingertip to discharge the static charge that had gathered, the sensor output would saturate and return to the previously calibrated state. Sensitivity would be increased for a short period of time (approx.. 20 sec) at which point sensitivity would begin to decrease until the electromagnetic field was no longer being detected by the sensors. Figures 32 – 34 are images of the oscilloscope during sensor calibration. The top line is the generated electric field signal. The lower line is the analog voltage output from the sensor.

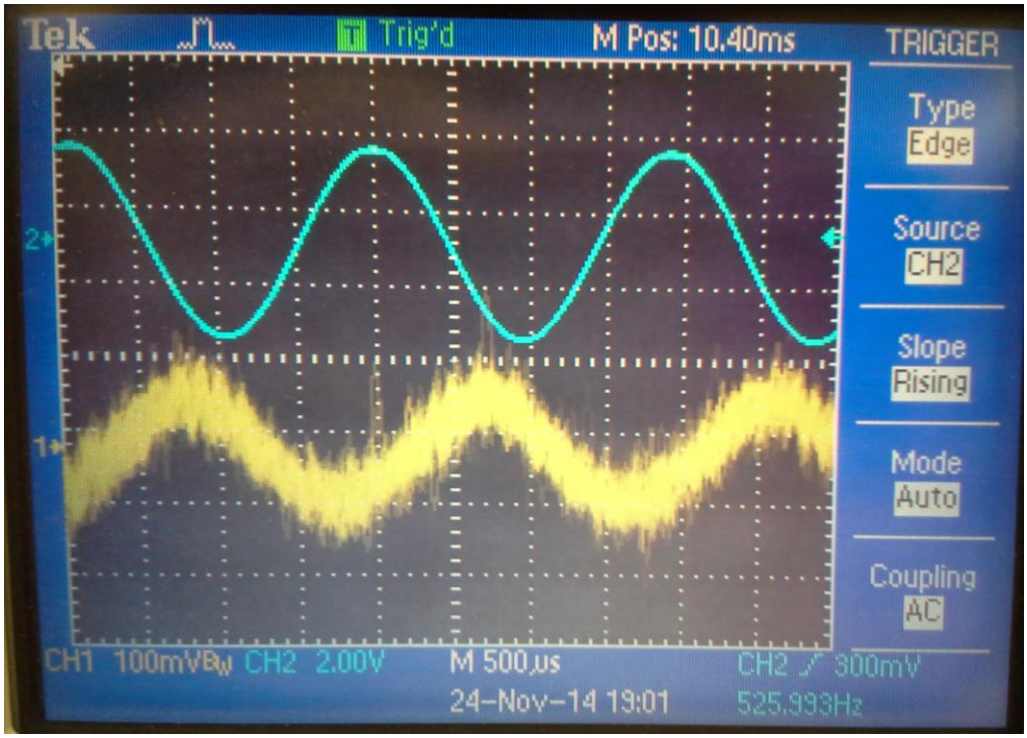

Figure 32: Sensor output 5 seconds after grounding

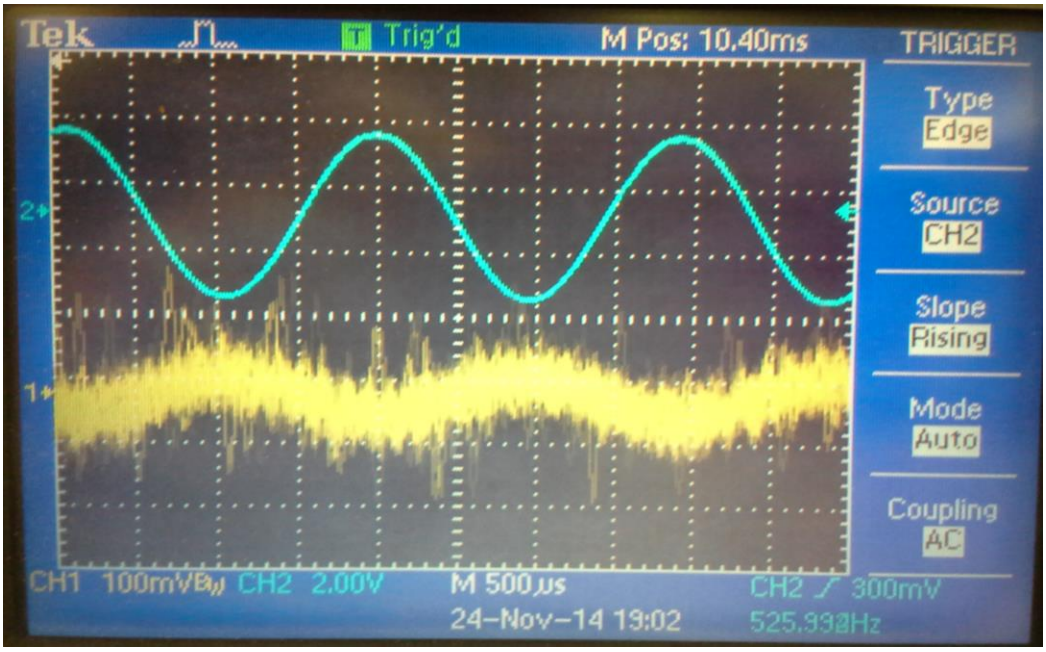

Figure 33: Sensor output 60 seconds after grounding

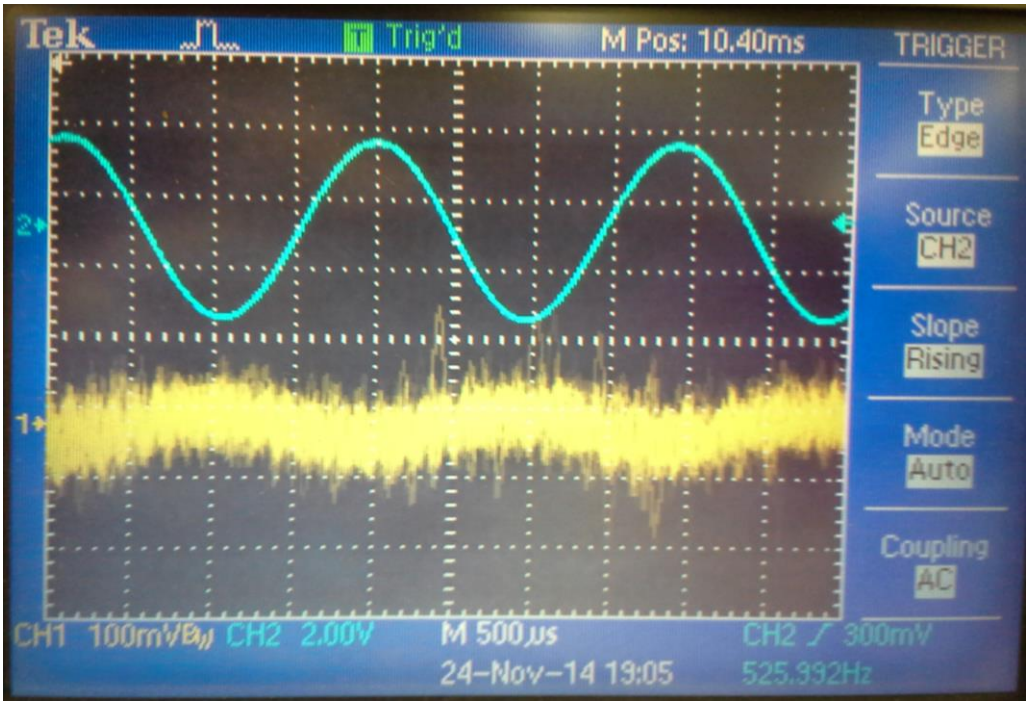

Figure 34: Sensor output 4 minutes after grounding

A possible solution for discharging the plates by touching them and then firing the low velocity projectile before sensor sensitivity decrease was tested. When this method was employed a 100% detection rate was recorded from the sensor. With this approach providing positive results, a solution for firing high velocity projectiles was evaluated. For safety reasons touching the plates prior to shooting high velocity projectiles was infeasible. This led to the employment of a 15 – 20 foot length of wire which was soldered to a paperclip. The paperclip was attached to the sensor plate, allowing effective discharging from a safe distance behind the muzzle. The sensor was discharged by grounding the exposed wires attached to the senor plates prior to the shooter firing, the wires were pulled, removing the paperclips from the sensors. The shooter would then fire and look for a successful trigger. Laboratory test were conducted to ensure that the paperclip method would sufficiently ground the sensors. The test provided a 100%

percent detection rate with the low velocity projectile. Figure 35 shows the test setup used for grounding.

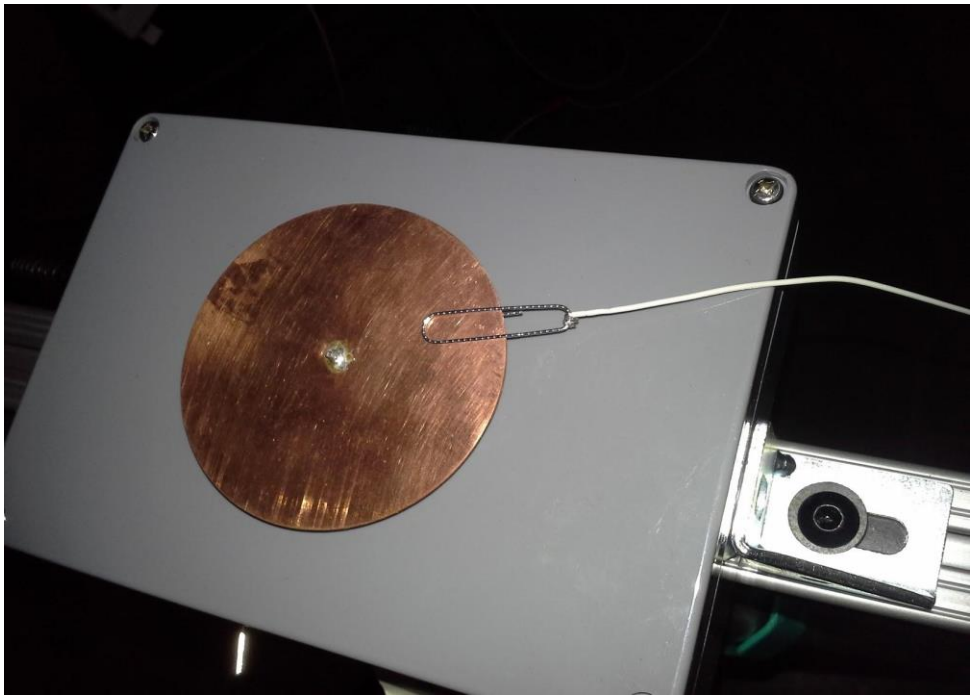

Figure 35: Grounding test setup

4.4 Field Refinement Results

The first test proved unsuccessful in producing a positive detection. This was partially due to the test being cut short when the second sensor plate was struck by a passing projectile on the third shot, the two prior shots had not produced a positive detection. This was purely the result of shooter error and not of the sensor.

It was noted that an optical chronograph would not function under the florescent lights of the indoor range.

After the sensor that was struck during testing was repaired and calibrated an outdoor testing session was conducted. Eight shots were fired with no positive detections

being recorded. Settings were verified at both the sensors and the oscilloscope being used and no abnormal settings were observed. APPENDIX C contains the data collection sheets from this test.

4.5 Indoor Sensor Analysis and Low Velocity Testing

The comparison between the old and current generation sensors provided the following insight. The signal noise level for the prior generation was greatly reduced in comparison with the current sensors. Prior generation sensor noise level average 0.02 volts compared to 0.04 volts for the current generation sensors. Fourier transform analysis was performed on the signal output noise in figures 36 and 38 using MATLAB software. The code used for analysis is displayed in APPENDIX D. Figure 37 is the results of the Fourier analysis for the current generation sensors used for all projectile testing. Figure 38 shows the results for the prior generation sensor that were used for detection testing in figure 13. All signals captured in this section have a sampling rate of 10 kSamples/s and were captured using an oscilloscope.

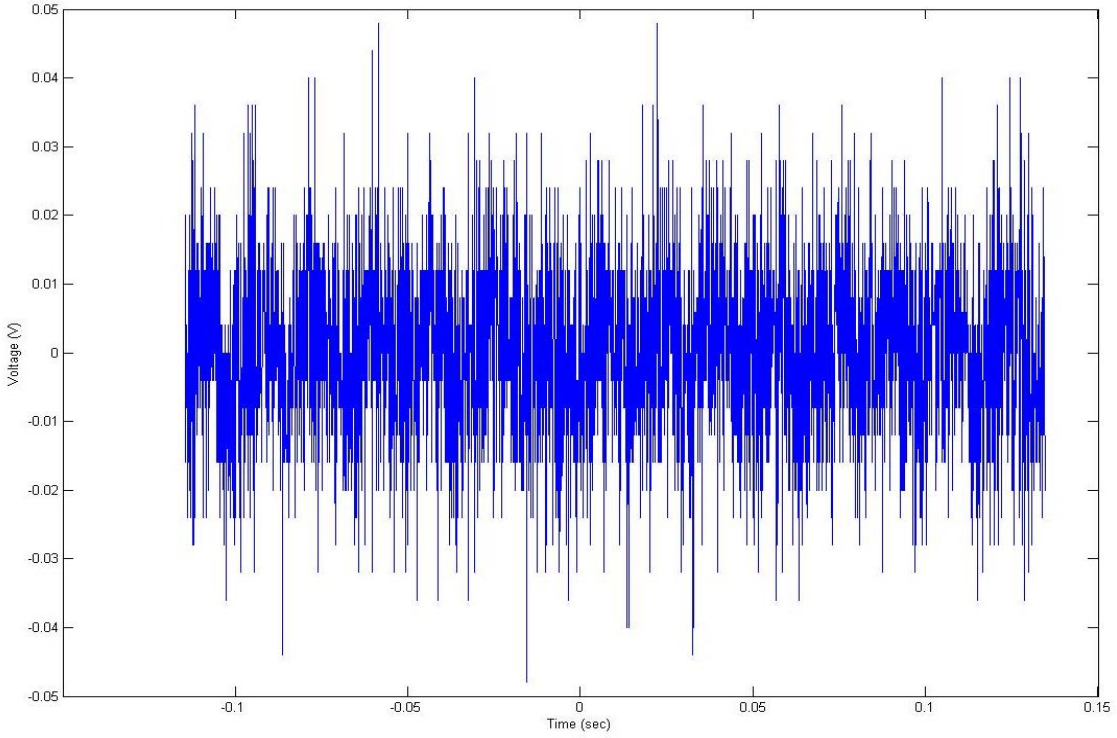

Figure 36: Current generation sensor noise

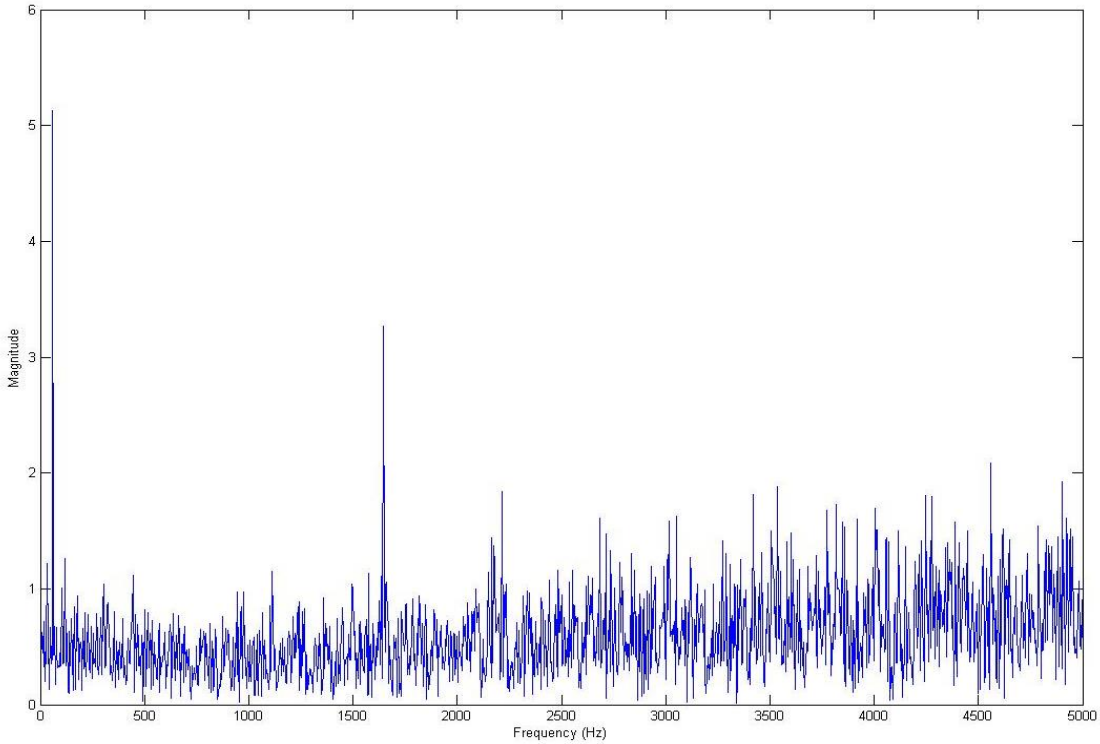

Figure 37: Current generation FFT

The Fourier analysis of the current generation signal noise identifies the signal as being created from a complex mix of frequencies inherent to the sensor. The largest components of the signal are identified by magnitude spikes at 60, 1645, 2215, and 4559 Hz.

In comparison the analysis conducted in figure 38 displays a clean signal with a small magnitude spike at 60 Hz. The magnitude spike near 0 HZ is indicative of DC off-set

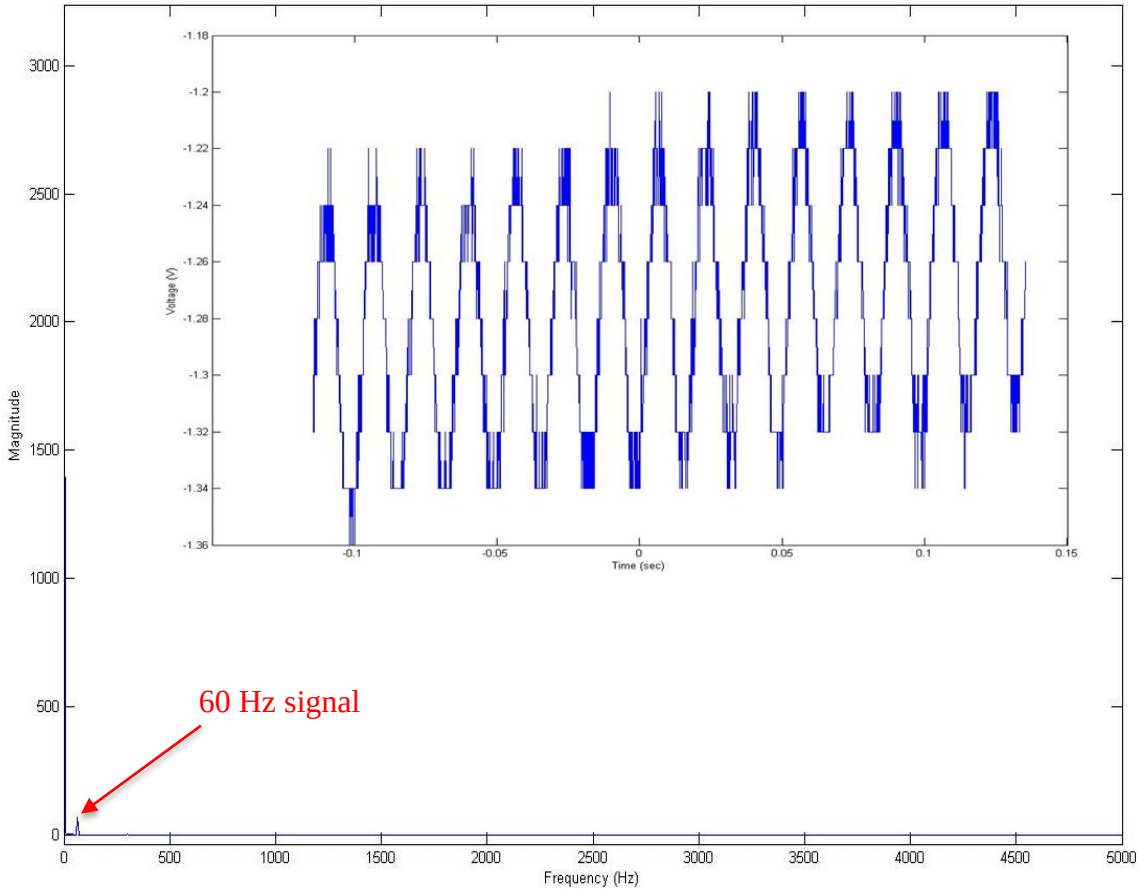

Figure 38: Prior generation FFT with sensor noise embedded

The results from firing low velocity projectiles over both sensors displayed the increased sensitivity of the older generation sensor. In the test 7 positive detections out of 10 attempts were recorded for the current generation sensor. The prior generation senor produced 12 positive detections in 12 attempts. Figure 39 and 40 are samples of the positive detections from the test.

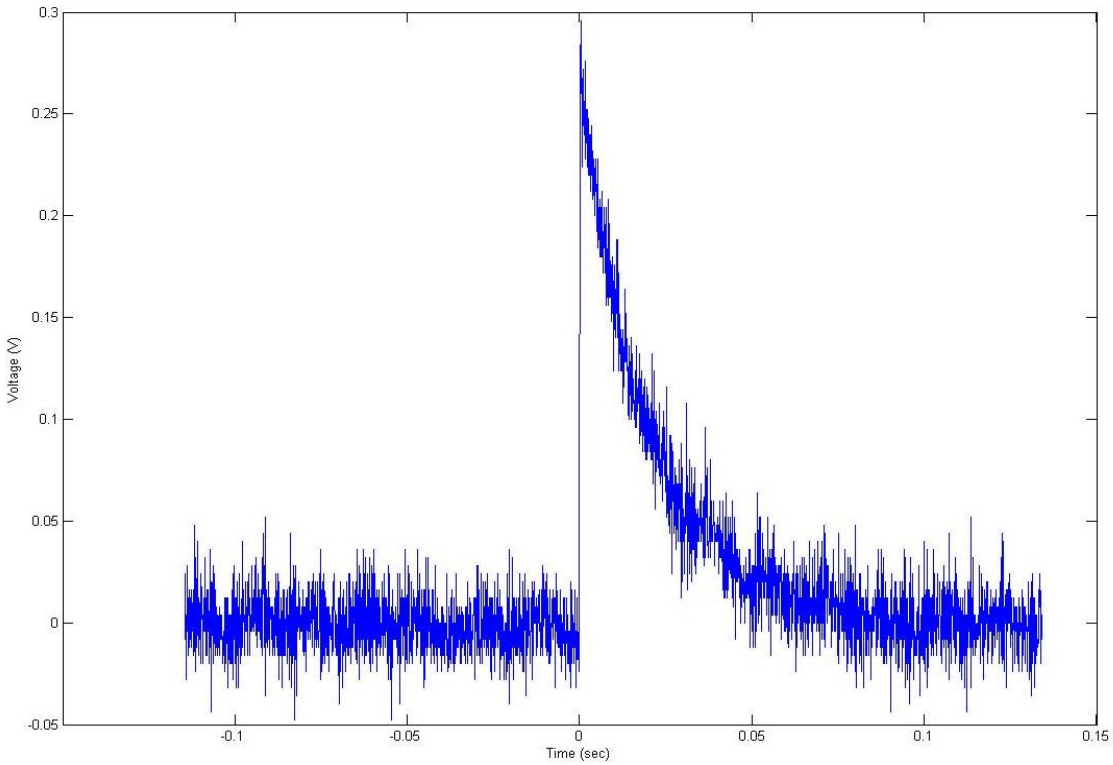

Figure 39: Current generation positive detection

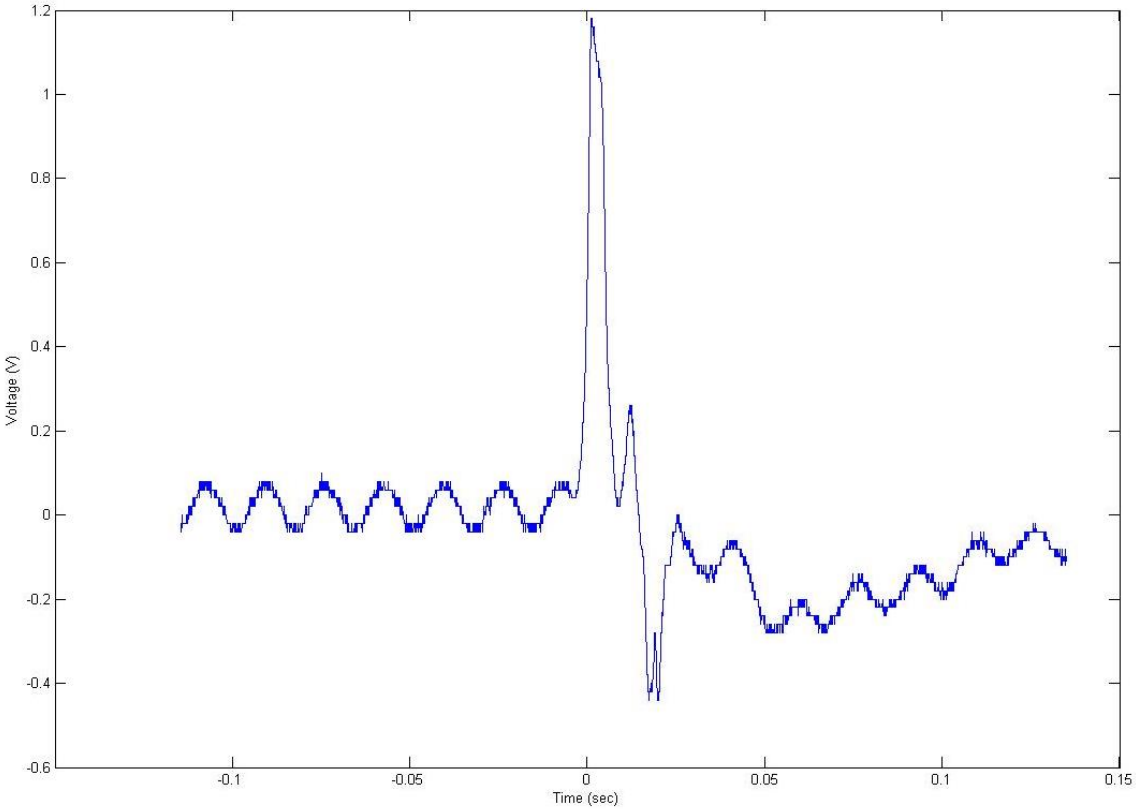

Figure 40: Prior generation positive detection

The prior generation sensor displayed increased consistency and detection voltages an order of magnitude higher than the current generation sensor.

CHAPTER 5: CONCLUSIONS

5.1 Feasibility Analysis

The sensors when functioning properly proved capable of detecting projectiles and providing accurate velocity readings in the supersonic region. This statement is confirmed by the results of the initial field testing. The combination of increased internal sensor noise and degradation in sensor detection ability that appeared as the current generation of sensor was continually tested prevented further testing in the transonic and subsonic regions.

Data collection resolution targeted at +/- 1% or higher velocity resolution should collect data at a minimum of 200k samples per second. Sampling at this rate or above will provide decreased error and provide highly accurate velocity readings.

Analysis of prior generation sensor produced positive detection results with increased voltage outputs and decreased signal noise when compared to current generation sensors. This analysis indicated that the internal differences between the previous and current generation is the cause of increased noise levels and decreased sensitivity.

5.2 Suggestions for Improvement

The solution appears to be remodeling the internal circuitry of the current generation sensors to closely mimic those of the first generation. The inclusion of some means of reliably bleeding static charge from the detection plate should also be included

in future models. This would insure that the sensors are constantly at peak sensitivity increasing the likelihood of detection.

5.3 Future Work

Using knowledge learned from the comparison of the two generations of sensors a high velocity test should be conducted to validate the performance of the prior generation sensor. This test would consist of employing the prior generation sensor as the trigger for data collection and a current generation sensor as the trailing sensor. An oscilloscope would provide the trigger and data collection capabilities. An optical chronograph should be used to record reference velocities. If the prior generation sensor preforms favorably this test would confirm the need to construct the next generation sensor with similar components.

REFERENCES

[1] Cortney, M., *Acoustic methods for measuring bullet velocity*. Applied Acoustics, 2008. **69**(10): p. 925-928.

[2] Hayden, R.D., *Sierra Reloading Manual*. 50th Anniversary ed. Vol. 4th. 1995, Sedalia: Sierra Bullets. 1040.

[3] Ingalls, J.M., *Ingalls' ballistic tables*. Rev. ed. 1918, Washington,: Govt. Print. Off. xxviii, 233p.

[4] Litz, B., *Applied ballistics for long range shooting*. 2009: Applied Ballistics.

[5] Mazurek, J.A., et al. *Boomerang mobile counter shooter detection system*. in *Defense and Security*. 2005: International Society for Optics and Photonics.

[6] McCoy, R. L. (1999). *Modern exterior ballistics: The launch and flight dynamics of symmetric projectiles*. Schiffer Pub., 1999.

[7] Nanevicz, J. and W. Wadsworth, *Measuring the electrical charge and velocity of a moving projectile*. 1965, DTIC Document.

[8] Noras, M.A. *Electric Field Sensor Based on a Varactor Diode/MIS/MOS Structure*. in *Industry Applications Society Annual Meeting (IAS), 2010 IEEE*. 2010.

[9] Noras, M.A., S.P. Ramsey, and B.B. Rhoades, *Projectile detection using quasi-electrostatic field sensor array.* Journal of Electrostatics, 2013. **71**(3): p. 220-223.

[10] Noras, M.A. "Solid State Electric Field Sensor", U. S. patent application no. 13/528,185, filed on June 20, 2012

[11] Sahu, J. (2008). Unsteady Free flight Aerodynamics of a Spinning Projectile at A High Transonic Speed" to the AIAA AFM Meeting. *Honolulu, HI*, 18-22.

[12] S.J. Vinci, D.M. Hull, Electrostatic Charge Measurements and Characterization of In-flight RPGs, in: Proceedings of the MSS Meeting on Battlefield Acoustic, Seismic, Magnetic, and Electric Field Sensors, 2004.

[13] P.A.M. Sandborn, S. Vinci, D. Hull, Bullet detection and localization using electric field sensors: distortion of sensed electric field by conducting sensor platforms, in: Proceedings of the MSS/BAMS Conference, 2010.

[14] http://images.doba.com/products/2330/images_acc_Competiton_Electronics_Prochrono_Digital_Chronograph_CEI_3800_lg.jpg

APPENDIX A: LABVIEW BULLET DETECTION VI

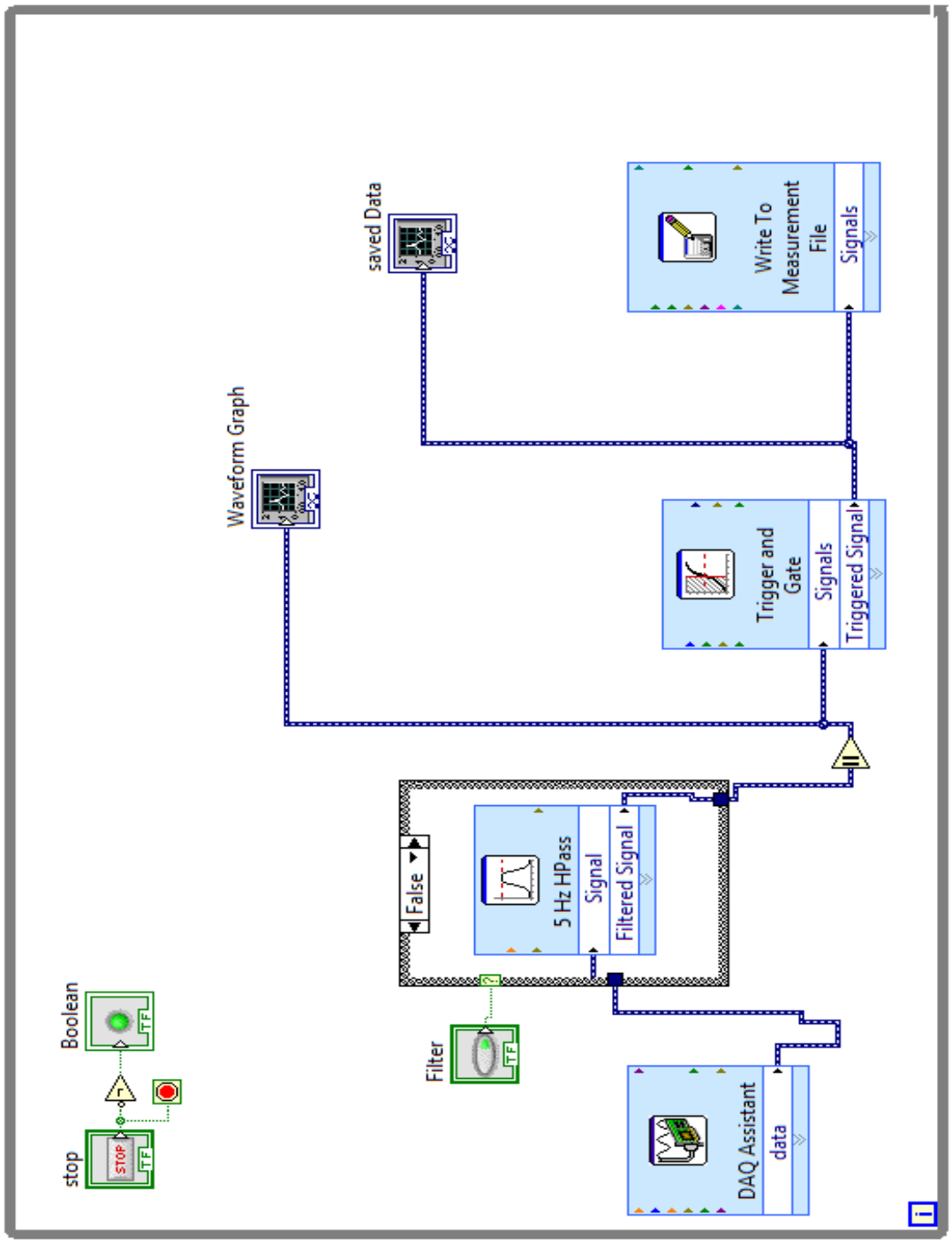

APPENDIX B: PEAK DETECTION / ERROR ANALYSIS MATLAB CODE

Peak Detection

```
[pks,locs]=findpeaks(Voltage_1Trigger,'minpeakheight',.6) %Finds Peaks and time based location that exceed the minimal peak height%
[pks,locs]=findpeaks(Voltage_0Trigger,'minpeakheight',.2) %Finds Peaks and time based location that exceed the minimal peak height%
plot(Time1, Voltage_0Trigger, Time1, Voltage_1Trigger)
```

Resolution and Error Analysis

```
dd=.0625/12; %distance error in feet%
dis=5; %Sensor distance in feet%
dismin=dis-dd; %Distance used for minimum velocity %
dismax=dis+dd; %Distance used for maximum velocity%
freq=(20000:5000:300000); %Frequency matrix%
error=1./freq; %Error matrix%
error2=2.*error; %Double error matrix%
error25=(0.002-error2); %Error matrix for 2500fps Vmax%
error25plus=0.002+error2; %Error matrix for 2500fps Vmin%
error30=(5/3000)-error2; %Error matrix for 3000fps Vmax%
error30plus=(5/3000)+error2; %Error matrix for 3000fps Vmin%
error35=(5/3500)-error2; %Error matrix for 3500fps Vmax%
error35plus=(5/3500)+error2; %Error matrix for 3500fps Vmin%
Vmax25=dismax./error25;
Vmin25=dismin./error25plus;
Vmax30=dismax./error30;
Vmin30=dismin./error30plus;
Vmax35=dismax./error35;
Vmin35=dismin./error35plus;
plot(freq,Vmax25,freq,Vmin25,freq,Vmax30,freq,Vmin30,freq,Vmax35,freq,Vmin35)
hold on
>> plot([0 300000],[2500 2500],'k-') %reference line at 2500fps%
>> plot([0 300000],[3000 3000],'k-') %reference line at 3000fps%
>> plot([0 300000],[3500 3500],'k-') %reference line at 3500fps%
>> hold off
```

APPENDIX C: FIELD REFINEMENT DATA SHEET

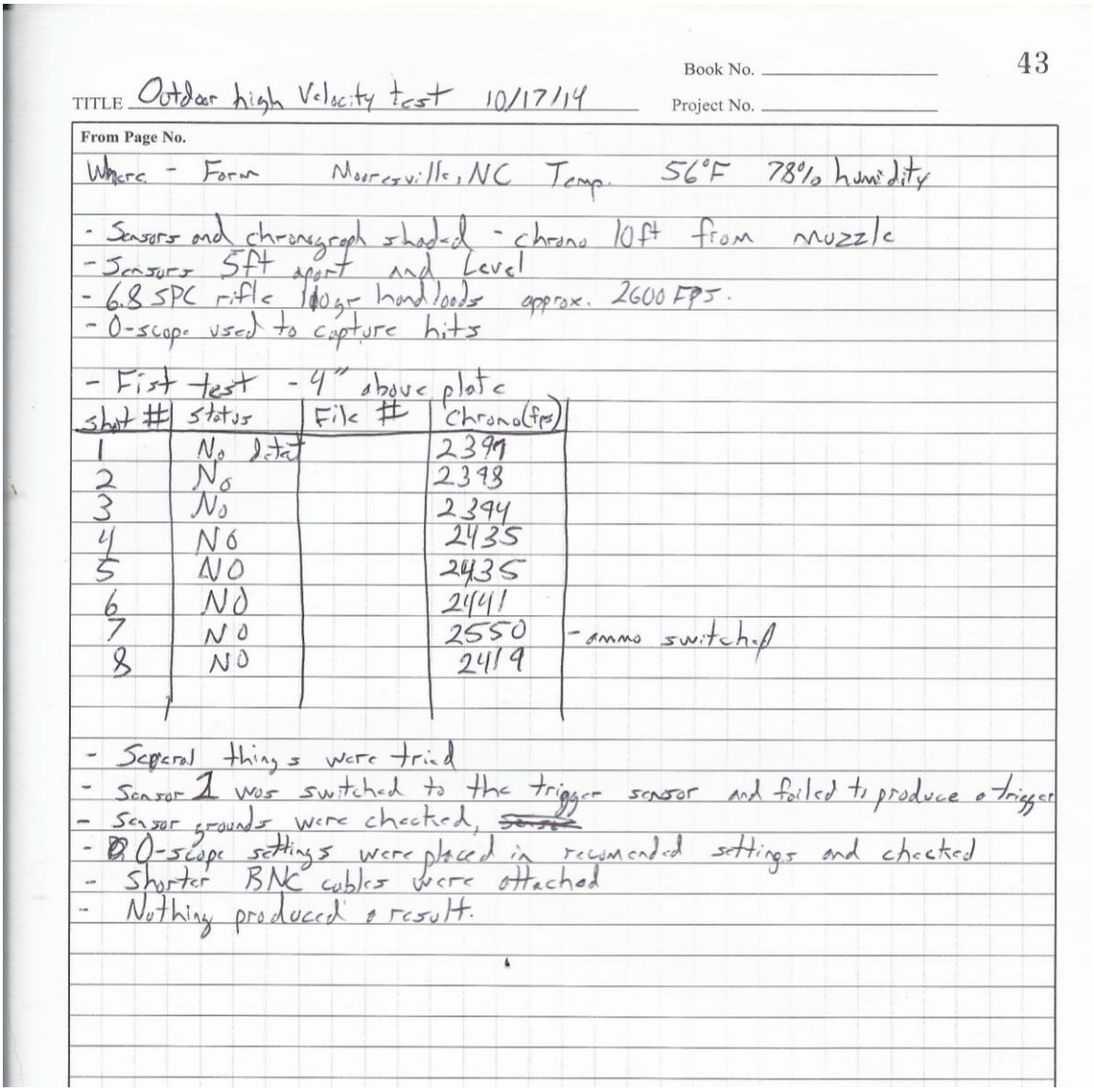

Book No. _____ 43

TITLE Outdoor high Velocity test 10/17/14 Project No. _____

From Page No.

Where - Form Mooresville, NC Temp. 56°F 78% humidity

- Sensors and chronograph shaded - chrono 10ft from muzzle
- Sensors 5ft apart and Level
- 6.8 SPC rifle 110gr handloads approx. 2600 FPS.
- O-scope used to capture hits

- Fist test - 4" above plate

shot #	status	File #	chrono(fps)	
1	No detect		2397	
2	No		2398	
3	No		2394	
4	No		2435	
5	No		2435	
6	No		2441	
7	No		2550	- ammo switched
8	No		2419	

- Several things were tried
- Sensor 1 was switched to the trigger sensor and failed to produce a trigger
- Sensor grounds were checked, ~~Sensor~~
- O-scope settings were placed in recommended settings and checked
- Shorter BNC cables were attached
- Nothing produced a result.

APPENDIX D: FAST FOURIER ANALYSIS MATLAB CODE

Signal analysis FFT

```
>> fs=200000; %Sampling rate samples/s%
>> N=58000; %Number of samples in the data%
>>  f=-fs/2:fs/(N-1):fs/2; %Frequency matrix at half sampes of fs%
>> z=fftshift(fft(Voltage_0Trigger)); %FFT of signal%
>> plot(f,abs(z)) %positve  plot of FFT magnitude vs frequency%
```